



Biogeochemical and redox record of mid–late Triassic reef evolution in the Italian Dolomites



Fabio Tosti ^{a,*}, Adelaide Mastandrea ^b, Adriano Guido ^b, Fabio Demasi ^b, Franco Russo ^b, Robert Riding ^a

^a Department of Earth and Planetary Sciences, University of Tennessee, 1412 Circle Dr., Knoxville, TN 37996, USA

^b Dipartimento di Biologia, Ecologia e Scienze della Terra, Università della Calabria, 87036 Rende, Italy

ARTICLE INFO

Article history:

Received 8 October 2013

Received in revised form 24 January 2014

Accepted 31 January 2014

Available online 9 February 2014

Keywords:

Biogeochemistry

Biomarkers

Carbonates

Dolomites

Reefs

Triassic

ABSTRACT

Geochemical signatures and carbonate microfacies highlight contrasts between two distinctive mid–late Triassic reef communities in the Dolomite Alps, Italy. In the first community, sponges, bryozoans, calcified cyanobacteria and problematic organisms (*Archaeolithoporella*, *Shamovella*), together with a variety of micritic fabrics, formed compact reefs in high energy shallow-water at the margins of high-rise Ladinian–Carnian carbonate platforms. Debris from these margins created steep foreslopes, and some large blocks of the allochthonous material (Wengen–Cassian formations, Cipit Boulders) were buried in basal shales that protected them from subsequent alteration and regional dolomitization. In the second and slightly younger community, small Carnian patch reefs (Heiligkreuz Formation, Alpe di Specie) developed in quieter shallow water, where they too were protected against alteration by enclosing shales. They were constructed mainly by scleractinian corals, sponges and red algae, and contain relatively large framework cavities with clotted-peloidal micrite. These early examples of coralgal reefs have broad similarities to present-day examples, whereas the community represented by the Cipit Boulders has more in common with Late Permian reefs.

Both bioconstructions preserve primary microfabrics and biomarkers. The Cipit Boulder samples contain bacterial, mainly cyanobacterial biomarkers, lack specific molecules typical of sulfate-reducing bacteria (SRB), and have Rare Earth Element (REE) values indicative of oxic conditions. These signatures are consistent with their original high-energy platform margin location, compact structure, and presence of calcified cyanobacteria such as *Cladogirvanella* and *Girvanella*. In contrast, the coralgal patch reefs contain SRB biomarkers, lack specific molecules typical of cyanobacteria, and have REE values indicative of sub-oxic conditions. These signatures are consistent with their lower energy depositional conditions and well-developed skeletal framework that created protected low-oxygen micro-habitats. The SRB biomarkers can be linked to the associated clotted-peloidal fabrics which resemble those commonly present in younger coral-reef frameworks. These details of redox conditions and bacterial processes underscore the important biotic, structural and environmental changes that affected shallow marine reefs during the Triassic.

© 2014 Elsevier B.V. All rights reserved.

1. Introduction

The late Permian to mid–late Triassic was an interval of profound change in reef development (Flügel and Stanley, 1984; Stanley, 1988; Flügel, 2002). Within a period of ~25 Ma, Permian-type reefs, dominated by sponges, bryozoans, calcified crusts and microbes, were replaced by more modern-looking reefs with scleractinian corals and calcareous red algae (Zankl, 1969; Stanley, 2003, 2006). The mid–late Triassic phase of this development is preserved in northern Italy where the Dolomite Mountains contain outstanding examples of reefal carbonates (Richthofen, 1860; Mojsisovics Von Mojvar, 1879; Ogilvie, 1893;

Salomon, 1895; Hummel, 1928; Pia, 1937; Leonardi, 1955, 1968; Bosellini and Rossi, 1974; Wendt, 1974; Fürsich and Wendt, 1977; Gaetani et al., 1981; Wendt, 1982; Bosellini, 1984; Hardie et al., 1986; Rudolph et al., 1989; Russo et al., 1991, 1997; Mastandrea et al., 1997; Gianolla, 1998; Kenter, 1990; Russo, 2005; Schlager and Keim, 2009; Stefani et al., 2010). These include remarkable Ladinian–Carnian high-rise platforms that prograded basinward over their marginal reef talus (Bosellini, 1984). Although many of these limestones were subsequently dolomitized, fragments thought to represent the platform margin reefs are locally exceptionally well-preserved (Wendt, 1974, 1975; Scherer, 1977; Russo et al., 1997) as meter-scale allochthonous blocks. The lithology and biota of these ‘Cipit Boulders’ contrast with those of younger small patch-reefs that are well-preserved in the late Julian Substage (Early Carnian) at the base of the Heiligkreuz/Dürrenstein Formation. These are dominated by a biota of calcified demosponges, scleractinian corals and calcified red algae that anticipates the ‘modernization’ of reef-building

* Corresponding author. Tel.: +1 865 684 0190.

E-mail addresses: ftosti@utk.edu (F. Tosti), amast@unical.it (A. Mastandrea), aguido@unical.it (A. Guido), fabio.demasi@unical.it (F. Demasi), francorusso44@gmail.com (F. Russo), rriding@utk.edu (R. Riding).

communities on a global scale between the Late Carnian and the Norian–Rhaetian (Fürsich and Wendt, 1977; Wendt, 1982; Russo et al., 1991; Flügel, 2002).

Very few studies have examined both Rare Earth Element (REE) and biomarker data in Phanerozoic reefs. We combined these approaches, together with carbonate microfacies analysis, to elucidate the depositional conditions and biogeochemistry of reef limestones during this period of mid–late Triassic transition. We compared samples of microbial-sponge reef limestones preserved in Cipit Boulders at Punta Grohmann (near Campitello di Fassa) that were derived from the last episode of widespread high rise platform development (Cassian Dolomite, ~225–229 Ma) in the area, with younger coral patch reefs in the Heiligkreuz Formation (~222 Ma) 40 km to the ENE at Alpe di Specie (Fürsich and Wendt, 1977; Russo et al., 1991, 1997; Russo, 2005) (Figs. 1, 2). We examined the organic matter preserved in these limestones, analyzed it for biomarkers, and analyzed REE values in the samples. We found evidence that the platform margin samples (Punta Grohmann) formed under oxic conditions and contain biomarkers for cyanobacteria, whereas the younger Alpe di Specie coral patch reefs formed under sub-oxic conditions and contain biomarkers for sulfate reducing bacteria.

2. Localities and samples

In the Dolomites, Ladinian–Carnian platforms prograded basinward over their marginal reef talus (Bosellini, 1984), and most of the Cipit Boulders are thought to be derived from their upper slopes or margins (Richthofen, 1860; Mojsisovics Von Mojvar, 1879; Leonardi, 1968; Wendt and Fürsich, 1980; Biddle, 1981; Russo et al., 1997; Gianolla et al., 1998; Gianolla and Neri, 2007). Accommodation space was significantly reduced during the Julian Substage and patch reefs developed at Alpe di Specie in the Heiligkreuz/Dürrenstein Formation (Russo et al., 1991; Keim et al., 2001; Stefani et al., 2004).

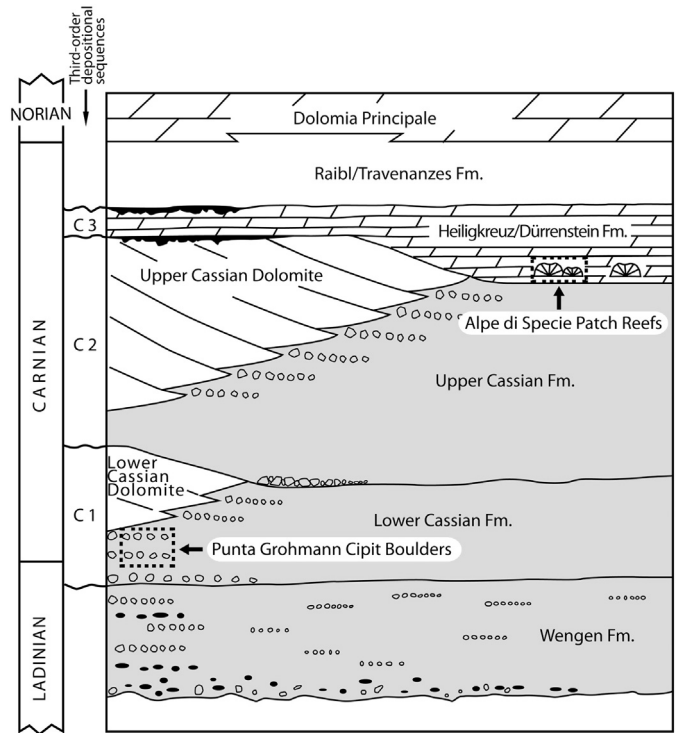


Fig. 2. Simplified stratigraphic scheme showing the mid-Triassic deposits sampled (dashed outlines). The contact between the Heiligkreuz/Dürrenstein Fm. and the Cassian Dolomite is thought to be erosional (Brandner et al., 2007). Modified from Preto and Hinnov, 2003; Keim et al., 2006.

2.1. Punta Grohmann

This Ladinian–Carnian basinal succession (Wengen and Cassian formations) is well-exposed on a steep shaly erosion scar (Teres Neigres)

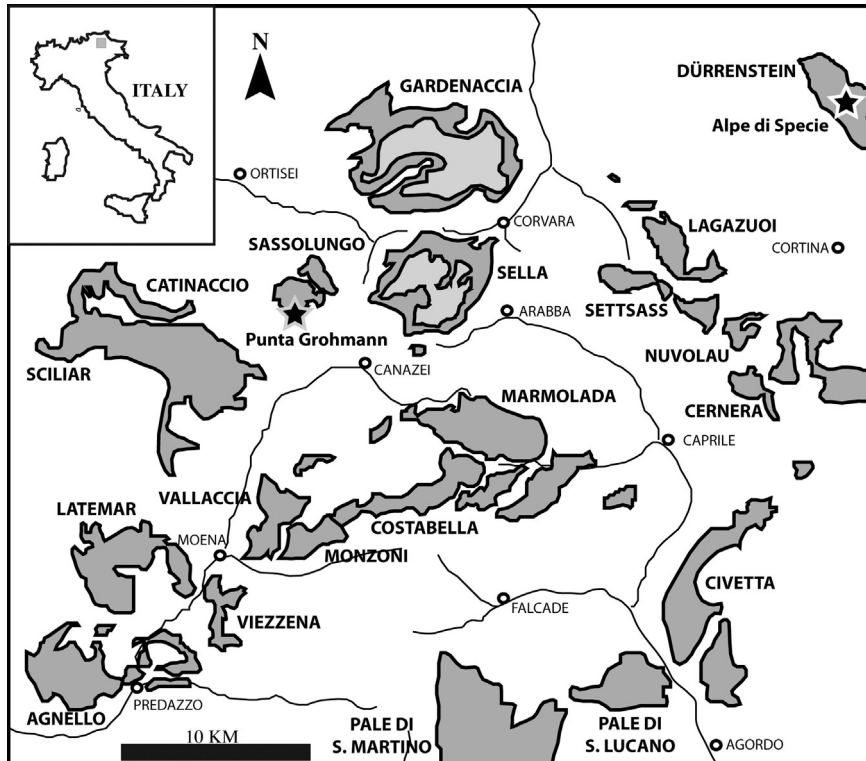


Fig. 1. Mid-Triassic carbonate platforms in the Dolomites and locations of the Punta Grohmann and Alpe di Specie sample localities. Based on Brandner et al., 2007.

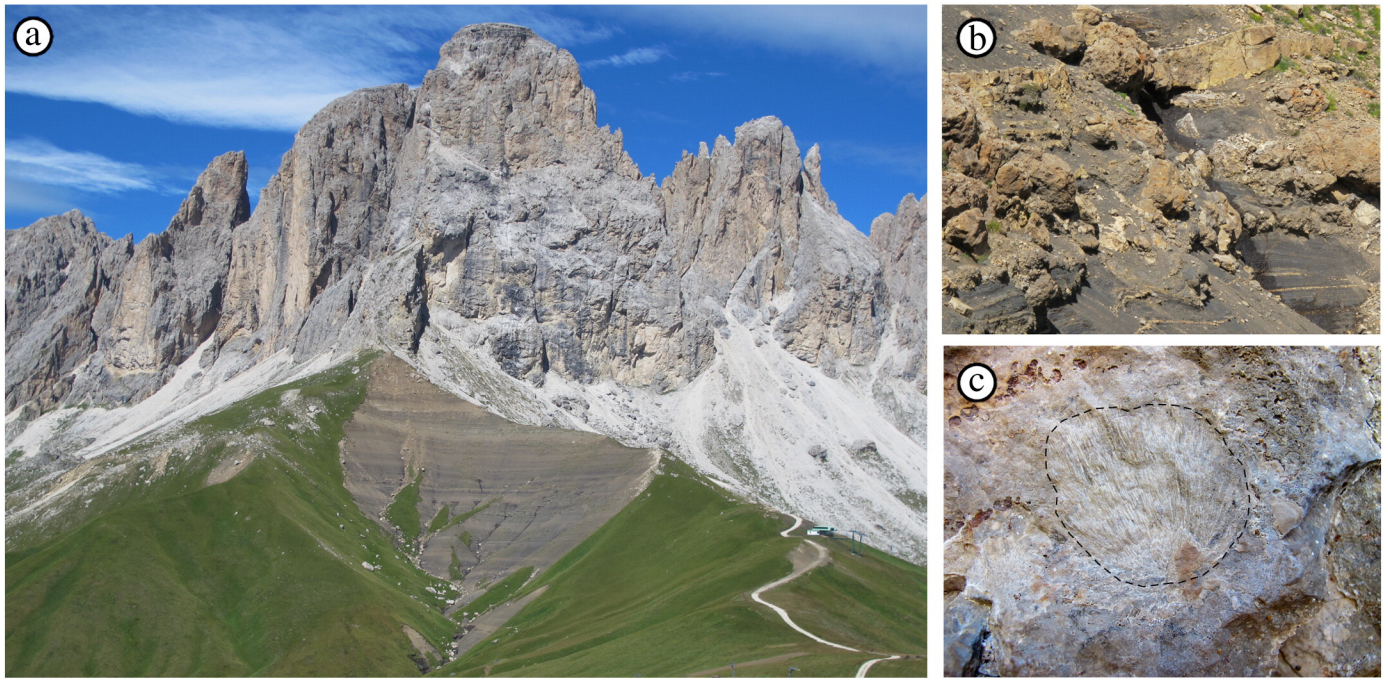


Fig. 3. a) Punta Grohmann locality viewed from the south-east. Punta Grohmann is the high peak in the center, which consists of clinoforms of Cassian Dolomite and marks the southern end of the Sassolungo mountain group. The shield-shaped gray erosion scar (Teres Neigres) below Punta Grohmann exposes the underlying basinal San Cassian Fm. of dominantly shale-mudstones with horizons of allochthonous margin-derived limestone blocks ('Cipit Boulders') from which our 'Punta Grohmann' samples were collected. Elevation of the gray exposure from base to top is ~250 m; and the top of the gray exposure to the top of Punta Grohmann is a further ~500 m; b) An 8 m thick megabreccia horizon of 'Cipit Boulders' within the San Cassian Formation about halfway up the gray erosion scar (Fig. 3a) and on its left-hand (SW) side; c) Detail of a Cipit Boulder in the lower part of the San Cassian Fm. (near the bottom of the view in Fig. 3a) showing the calcified cyanobacterium *Cladogirvanella* (outlined) in reef limestone; width of view 8 cm.

(Fig. 3a) immediately below Punta Grohmann peak, at the southern edge of the Sassolungo/Langkofel group, 30 km east of Bolzano (Fig. 1). The Wengen Fm./Cassian Fm. succession is ~550 m thick and consists mainly of basinal terrigenous and volcanoclastic sediments with gravity displaced carbonates (Fig. 3b, c). Pillow lavas and heterogeneous breccias of the Fernazza Fm. are erosionally overlain by the 320 m thick Wengen which has volcanoclastic conglomerates at its base followed by volcanoclastic turbiditic sandstones and dark pelites. The ~50 m thick middle part of the Wengen contains horizons rich in platform-derived blocks of reef limestone (Richthofen Von, 1860; Ogilvie Gordon, 1927, 1929; Leonardi, 1968; Scudeler Baccelle, 1971; Assereto et al., 1977; Wendt and Fürsich, 1980; Bosellini, 1984; Russo et al., 1997; Giannolla et al., 1998, 2010; Giannolla and Neri, 2007; Mietto et al. 2012, Fig. 6). These were named Kalkstein von Cipit by Richthofen Von (1860), after the Rio Cipit/Tschapit Bach locality in the Alpe di Siusi area, 10 km west of Punta Grohmann. The Wengen–Cassian contact has been variously defined. Here we follow Russo et al. (1997, Fig. 2). In this view, the Wengen Fm. is overlain by the 220 m Cassian Fm. which shows a general coarsening upward trend and contains brown and yellowish marls. Platform-derived centimetric to metric size Cipit Boulders are especially abundant near the base of the overlying Cassian Dolomite carbonate platform. We sampled twenty Cipit Boulders of various sizes: ten from three horizons (U1, U2, U3) in the upper Wengen Fm., and ten from two layers (U4, U5) in the Cassian Fm. (Fig. 2).

2.2. Alpe di Specie

The rich and excellently preserved Carnian reef fauna at Alpe di Specie, 12.5 km NNE of Cortina D'Ampezzo, has attracted numerous studies (Loretz, 1875; Ogilvie, 1893; Pia, 1937; Dieci et al., 1970; Fürsich and Wendt, 1977; Russo et al., 1991; Neuweiler and Reitner, 1995; Sánchez-Beristain et al., 2011) although interpretation of these deposits is hindered by poor exposure. They have generally been regarded as small patch reefs that are either in situ (Ogilvie, 1893) or out of place (Fürsich and Wendt, 1977; Wendt, 1982; Russo et al., 1991). They have

also been regarded as 'Cipit Boulders' within the Cassian Fm., and therefore as downslope displacements from the Cassian Platform (Neuweiler and Reitner, 1995; Sánchez-Beristain et al., 2011). However, although probably somewhat displaced, most studies have regarded them as less far-traveled than Cipit Boulders. Wendt (1982) thought they were displaced from the uppermost Cassian Fm., whereas Russo et al. (1991) considered them to have moved within the lowest 8 m (Member A) of the overlying Dürrenstein/Heiligkreuz Formation. Meter-scale patch reefs (Fig. 2) elsewhere at this level (also termed the Borca Member, Stefani et al., 2004, p. 44) have been regarded as more-or-less in situ (e.g., Preto and Hinnov, 2003; Neri et al., 2007). Nonetheless, in common with Cipit Boulders, the Alpe di Specie mounds/erratics have been protected from alteration and regional dolomitization by the surrounding shaly sediments (Scherer, 1977; Wendt, 1977, 1982; Russo et al., 1991).

Dürrenstein/Heiligkreuz deposition marked a change from the prograding and at times high-rise rimmed carbonate platforms of the late Ladinian–early Carnian (Bosellini, 1984; De Zanche et al., 1993) to carbonate ramp (Preto and Hinnov, 2003) and restricted, locally anoxic, basin (Keim et al., 2006) conditions. This mixed terrigenous-carbonate succession onlaps the Cassian platform slope and unconformably overlies the platform top (Preto and Hinnov, 2003, Fig. 2), reflecting a complex series of events, possibly in part climate-driven (Bosellini, 1984; Hardie et al., 1986; Stefani et al., 2010). Ten samples from five different patch reefs were collected from Member A of the Heiligkreuz/Dürrenstein Fm. (Fig. 2). The Cassian to basal Dürrenstein/Heiligkreuz contact is within the *Austriacum* ammonoid biozone (Gianolla et al., 1998; De Zanche et al., 2000) and Member A is close to the overlying Juvalian–Tuvallian boundary (Car3) (Stefani et al., 2004).

3. Methods

We examined a total of 30 rock samples, 20 from Punta Grohmann and 10 from Alpe di Specie. After initial screening by optical microscopy and UV epifluorescence to determine the best-preserved samples suitable for further analyses, we selected 12 samples that were individually

crushed and homogenized prior to analyses for Total Organic Carbon content, presence of major functional groups, biomarkers and Rare Earth Element (REE) concentrations.

3.1. Optical microscopy: petrography and epifluorescence

Micro- and nano-morphologic examination and localization of organic compounds was performed by optical and UV epifluorescence microscopy on polished thin-sections (3×2.5 cm in size, ~ 35 μm thick). Fluorescence was induced by an Hg vapor lamp linked to an Axioplan II microscope (Zeiss) equipped with wide bandpass filters (BP 436/10 nm/LP 470 nm for green light; BP 450–490 nm/LP 520 nm for yellow light).

3.2. Total Organic Carbon (TOC)

Samples were thoroughly washed in distilled water, and the outer-most portions removed and discarded. The samples were ground in an agate mortar to a fine powder. TOC data were obtained with a UIC CM135 TC/TOC Analyzer at the Department of Earth and Planetary Sciences, University of Tennessee, Knoxville. Using porcelain “boats”, part of the powder (~ 15 mg) of each sample was placed in a high temperature (950 °C) furnace with an oxygenated atmosphere. The Total Carbon (TC) was rapidly oxidized to CO_2 and any reaction products (sulfur oxides, halides, water, nitrous oxides, etc.) were removed by the post-combustion scrubbers. The resulting carbon dioxide was then swept into a UIC CM5015 CO_2 Coulometer where its concentration was automatically measured using absolute coulometric titration. In order to evaluate Total Inorganic Carbon (TIC) the powder samples were acidified and purged of carbonate carbon, the released CO_2 was swept into the colorimeter cell to measure its concentration. The TOC was calculated by: $\text{TOC} = \text{TC} - \text{TIC}$.

3.3. Extract preparation for organic analyses

Following Logan and Eglinton (1994), with minor modifications by Guido et al. (2012a), extraction was carried out on 100 g of powder using a mixture of dichloromethane/methanol (1:1, v:v) by ultrasonication. The supernatant liquid, separated from the powder by centrifugation, was collected in a clean vial. The extraction procedure was repeated three times. The collected liquid constituted the total lipid fraction which was first analyzed by Fourier Transform-Infrared Spectroscopy (FT-IR) to obtain overall characterization of organic functional groups and evaluate sample preservation. For biomarker analyses, total lipid extracts were fractionated by solid phase extraction performed with AminoPropyl Bond Elute® cartridges, using solvents of increasing polarity. Extracts were dried under nitrogen flux. Acidic compounds were eluted with ether, after acidification of the medium with ether:formic acid (9:1). Before analysis, fatty acids were esterified using acetyl chloride in anhydrous methanol. The hydrocarbon fraction was separated from the neutral fraction by flash chromatography on deactivated silica (5% water) by eluting with heptane. Neutral compounds were eluted with dichloromethane/methanol (1:1).

3.4. Fourier Transform-Infrared Spectroscopy (FT-IR)

FT-IR spectroscopy was performed in the mid-infrared area (4000 – 400 cm^{-1}) using a Perkin Elmer Spectrum 100 Spectrophotometer with a Universal ATR (Attenuated Total Reflectance) with a K–Br beamsplitter and a LiTaO₃ detector, with a resolution of 4 cm^{-1} . A few drops of the total lipid extract were placed on the crystal of the ATR apparatus and dried under nitrogen flow. Spectral bands were assigned according to the literature (Painter et al., 1981; Wang and Griffiths, 1985; Solomon and Carangelo, 1988; Sobkowiak and Painter, 1992; Mastandrea et al., 2011; Guido et al., 2012a,b, 2013a,b). A Factor ($(2930 + 2860 \text{ cm}^{-1}) / (2930 + 2860 + 1630 \text{ cm}^{-1})$) and C Factor

($(1710 \text{ cm}^{-1}) / (1710 + 1630 \text{ cm}^{-1})$) were measured to classify the kerogen types and maturation level of the organic compounds. These factors, used in a similar manner to the traditional H/C–O/C elemental ratios and to Rock-Eval pyrolysis parameters, such as Hydrogen Index (HI)–Oxygen Index (OI), are useful in quantifying changes in the abundance of aliphatic and carbonyl/carboxyl groups and can be utilized to differentiate marine and continental sources (Ganz and Kalkreuth, 1987; Guido et al., 2012a,b, 2013a,b).

3.5. Gas chromatography–mass spectrometry (GC-MS)

Molecular compounds were identified by GC/MS using a Varian Saturn 2000 instrument in the Department of Chemistry, University of Calabria, equipped with a Varian Factor Four-5MS capillary column ($30 \text{ m} \times 0.25 \text{ mm}$ i.d., $0.25 \mu\text{m}$ film thickness, crosslinked 5%-diphenyl–95%-dimethyl siloxane). Helium was used as the carrier gas at a linear flow velocity of 1.1 ml/s. The temperature was held at 40 °C for 1 min, then increased from 40 to 120 °C at 30 °C min^{-1} , and 120 to 300 °C at 5 °C min^{-1} , with the final isothermal hold at 300 °C for 20 min. The sample was injected unsplit, with an injector temperature of 280 °C. Squalane was added as an internal standard. The MS was operated in the electron impact mode at an ion trap temperature of 230 °C and emission current of 10 mA. Compounds were identified by comparison with published mass spectra and relative retention times (Bartle et al., 1979; Tissot and Welte, 1984; Baranger and Disnar, 1988; Baranger et al., 1989; Russell et al., 1997; Thiel et al., 1997; Peters et al., 2005a,b; Guido et al., 2007; Heindel et al., 2010; Tosti et al., 2011a, 2012; Guido et al., 2013c).

3.6. Rare Earth Elements

Sample preparation (decalcification) and the protocol for obtaining Rare Earth Element and Yttrium (REE + Y) distribution patterns follow those of Eggins et al. (1997) as modified by Mastandrea et al. (2010) and Guido et al. (2011). Twelve samples were broken into millimeter-size fragments and ground to powder. Using a Mars5 apparatus (CEM technologies) and teflon (TFM) digestion vessels, 100 mg of powder from each sample was dissolved in a mixture of hydrofluoric acid (2 ml HF), nitric acid (8 ml HNO_3) and perchloric acid (2 ml HClO_4). Before complete evaporation of the acid, 2 ml of perchloric acid was added to ensure complete removal of the hydrofluoric acid. Mother solutions were obtained by allowing the reaction solutions to cool slowly and then diluted to 100 ml with millipore water up to a sample/solution weight ratio of 1:1000. Trace element concentrations were determined using Perkin-Elmer Elan DRc Inductively Coupled Plasma-Mass Spectrometry (ICP-MS) in the Department of Earth Science, University of Calabria. The same procedures were used to prepare two standard reference materials: Dolomitic Limestone (SRM 88b) from N.I.S.T. and Micaschist (SDC-1) from the US Geological Survey. These were used as unknown samples during the analytical sequence (Eggins et al., 1997). REE + Y concentrations were determined by external calibration curves, prepared using Perkin Elmer “multi-element Calibration Standard 2 solution”. Internal standards (Indium, Germanium, Rhenium) were added to standards and solutions. In total, 24 analyses comprising 12 unknown determinations, 8 quality control standards (Limestone and Micaschist), and 4 blank determinations, were combined during the analytical run. To evaluate accuracy, the mean values of measurements carried out on the quality control standards were compared with those certified. Accuracies were better than 8%, with most elements within $\pm 5\%$. The instrument detection limit was evaluated by multiplying the standard deviation of the blanks by 3. The REE + Y distributions for the samples are shown as normalized REE + Y patterns in which Y is inserted between Dy and Ho according to ionic radius (Bau and Dulski, 1996). In addition to REE content, quantitative evaluation of the positive La anomaly and negative Ce anomaly in the shale-normalized REE + Y patterns was used to assess depositional conditions

(Bau and Dulski, 1996; Kamber and Webb, 2001). Because these two anomalies are related, they are commonly plotted in a PAAS-normalized diagram of $(La/La^*)_{sn}$ vs $(Ce/Ce^*)_{sn}$ where $La^*_{sn} = Pr_{sn} + 2 \times (Pr_{sn} - Nd_{sn})$ and $Ce^*_{sn} = Pr_{sn} + (Pr_{sn} - Nd_{sn})$ (Lawrence et al., 2006). Since Pr in Alpe di Specie samples presents a negative anomaly and could influence Ce evaluation, the algorithms were modified using Nd and Sm as follows: $La^*_{sn} = Nd_{sn} + 3 \times (Nd_{sn} - Sm_{sn})$ and $Ce^*_{sn} = Nd_{sn} + 2 \times (Nd_{sn} - Sm_{sn})$.

4. Results

4.1. Microfacies

4.1.1. Punta Grohmann

Punta Grohmann samples have a distinctive skeletal-microbial boundstone fabric with stromatolitic, peloidal and aphanitic micrites (Fig. 4a), calcified cyanobacteria (*Girvanella*, *Cladogirvanella cipitensis*, Fig. 5a) and problematic calcified organisms such as *Shamovella* (Fig. 5b), *Archaeolithoporella* sp., *Plexoramea cerebriformis*, *Macrotubus*

babai, and *Baccanella floriformis*. These small (up to a few mm) encrusting and baffling microorganisms are intimately associated with the micritic microbial crusts and botryoidal and fibrous cements, which fill small vugs and stromatactis-like cavities. Common demosponges include *Solenolmia manon* (Fig. 5c). Late cements occluding residual cavities are blocky ferroan sparry calcite. Bright epifluorescence commonly associated with the presence of calcimicrobes, micritic crusts and some aphanitic micrites, indicates high concentrations of organic matter.

4.1.2. Alpe di Specie

Small (<5 m) coralgal patch reefs (Fig. 4b), consisting mainly of centimetric scleractinian corals (e.g., *Margarosmia* sp., Fig. 6a), sponges (*Amblyisiphonella* sp., *Cryptocoelia zitteli*, *Uvanella irregularis*; *Atrochaetetes medius*; *Colospongia andrusovi* (Fig. 6b)) and calcareous red algae (*Solenopora* Fig. 6c, *Dendronella*), developed in the relatively muddy low-energy environment of Alpe di Specie. They form a complex framework (Fig. 7), poor in early cement, in which the cavity system represents 35% of the overall mound sediment. Despite the small size of the individual skeletons, the framework accreted sufficiently fast to

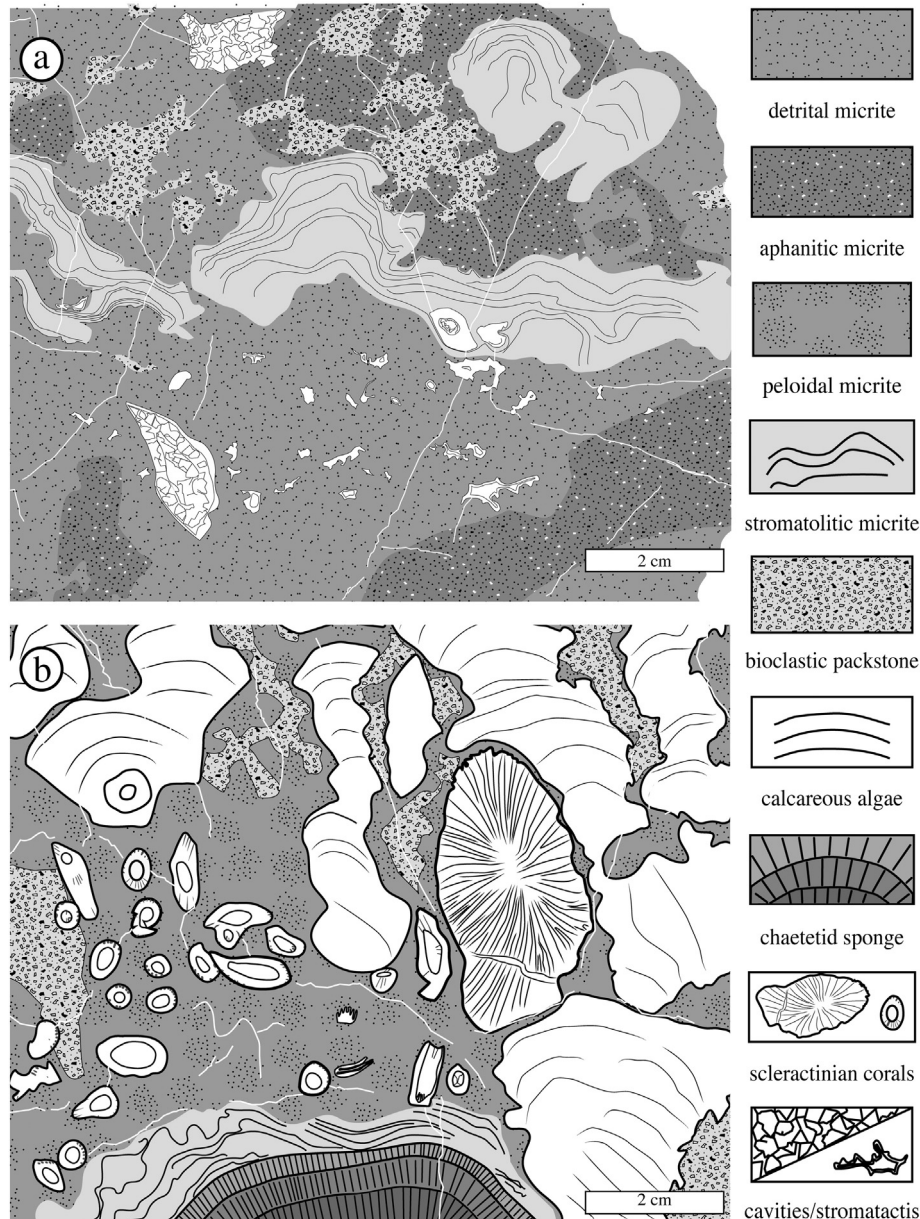


Fig. 4. Sketches of (a) Punta Grohmann and (b) Alpe di Specie reef fabrics.

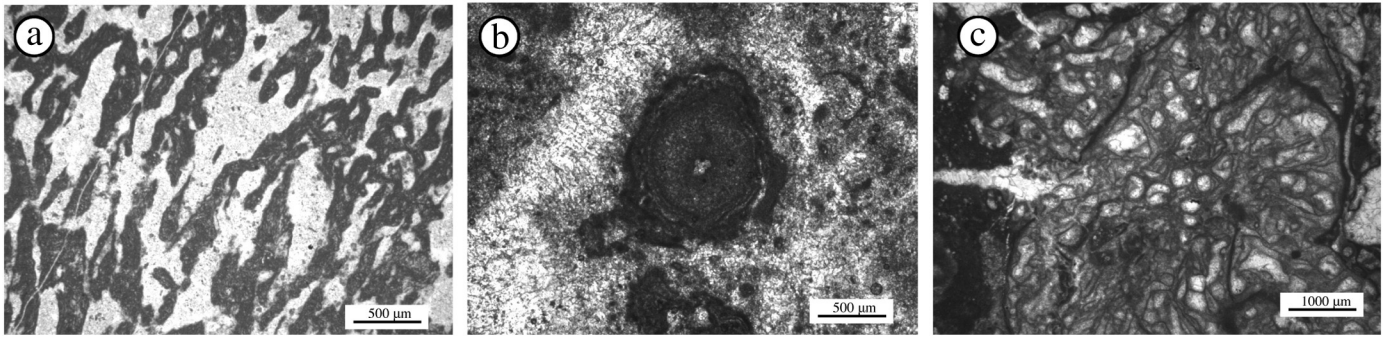


Fig. 5. Transmitted light microphotographs of Punta Grohmann Cipit Boulder specimens: a) *Cladogirvanella* sp., sample PG1; b) *Shamovella* sp., sample U3; c) *Solenolmia manon*, sample U1.

maintain relief above the adjacent substrate. Bright fluorescence, indicating high organic compound content in the peloidal micrite (as well as in the metazoan skeletons), supports an autochthonous bacterial interpretation of the micrites in these coral-algal reefs. This reasoning was also applied by Cuif et al. (1990) and Müller-Wille and Reitner (1993) in studies of residual organic matter in carbonates and biomineralization processes in sphinctozoan sponges. Similarly, Russo et al. (1997) distinguished autochthonous and allochthonous micrites in samples from the Cassian Formation and used bright autofluorescence in stromatolitic laminites and thrombolites to infer microbially-induced mineralization processes.

4.2. Total Organic Carbon (TOC) and FT-IR analyses

TOC concentration in the Punta Grohmann samples ranges from 0.5 to 1.5%, with an average of ~1% (Fig. 7). Samples U3, U4 and U5 show above-average concentrations. All the values are higher than those reported from Lower Triassic shallow water carbonates in Japan (average of ~0.08; Musashi et al., 2001) and from Gartnerkofel in Austria (0.05–0.15%; Magaritz et al., 1992), but are similar to Late Triassic carbonates of the Kossen Fm., Austria (0.11–1.50%; McRoberts et al., 1997) and the Eiberg Basin, Austria (average of ~1%; Ruhl et al., 2009). Low Early Triassic organic carbon concentrations are consistent with a declining trend near the Permian–Triassic Boundary (PTB) that suggests reduced primary productivity (algae, cyanobacteria) and/or increased organic matter degradation (Morante and Hallam, 1996). Following the PTB, a sharp increase in C_{org} (0.1%–0.3%) in limestones in western Slovenia (Schwab and Spangerberg, 2004) has been linked to higher primary productivity due to increased pCO_2 or other nutrient supply. TOC values similar to Punta Grohmann have also been recorded in the upper Triassic Meride Limestone Formation (average of 1%, Bernasconi and Riva, 1993; Mattavelli et al., 1993; Picotti et al., 2007) from northern Italy and in pre-Jurassic carbonate source rocks (0.03–1.59%, average of 0.3%, Yin et al., 2011) and calcified microbial framestones (0.6–5.8%, average: 2.7%, Krull et al., 2004), both in South China.

FT-IR analyses of total lipid extracts, following the procedure described above, show spectral bands in the range 600 to 3000 cm^{-1} . They contain methyl and methylene [$\delta(CH_2 + CH_3)$; 1458 cm^{-1}] groups, stretching aliphatic bands ($\nu CH_{2/3}$) (2949, 2918 and 2848 cm^{-1}), and methyl deformation bands (δCH_3 ; 1365 cm^{-1}). The spectra also display bands assigned to carbonyl and/or carboxyl groups ($\nu C=O$; 1740 cm^{-1}) and to the skeletal vibration of more than four methylene groups [$\delta(CH_2)_4$; 720 cm^{-1}]. The $\nu C-O$ vibration, between 1300 and 1100 cm^{-1} , and the $\nu C=C$ band were also recorded. Thermal maturity was evaluated using standard geochemical parameters, such as A and C factors (Ganz and Kalkreuth, 1987). All Punta Grohmann samples fall within the catagenesis field, implying good preservation of organic matter, consistent with the optical and epifluorescence observations.

Higher TOC concentrations (1–2.5%, average of ~2%) were recorded in the Alpe di Specie samples (Fig. 8). Similar TOC values occur in Late Triassic shallow marine micritic coral bioherms from Alaska that show a maximum concentration of 5.3%, an average of 1.53%, with more than 10 samples >2% (Whalen and Beatty, 2008). FT-IR analyses of Alpe di Specie samples record similar functional groups to those of Punta Grohmann, with aliphatic, carbonyl/carboxyl and double carbon bond stretching vibrations, but different relative abundances. The aliphatic C–H stretching region (3000 to 2800 cm^{-1}) presents three spectral bands: at 2955 cm^{-1} (asymmetrical CH_3 stretching), 2925 cm^{-1} (asymmetrical CH_2 stretching) and 2850 cm^{-1} (symmetrical CH_2 stretching), with lower absorption intensities at Alpe di Specie compared with Punta Grohmann. The C=O and C=C stretching bands show the same behavior. The A and C factors indicate that Alpe di Specie organic matter maturity has values in the diagenesis field (see Ganz and Kalkreuth, 1987) and therefore has better preservation than Punta Grohmann samples (Fig. 9). Overall, these maturity data agree with the optimal preservation of the carbonates in both successions.

4.3. Biomarker analyses

Mainly even numbered, straight-chain, saturated carboxylic acids, were detected in both Punta Grohmann and Alpe di Specie samples.

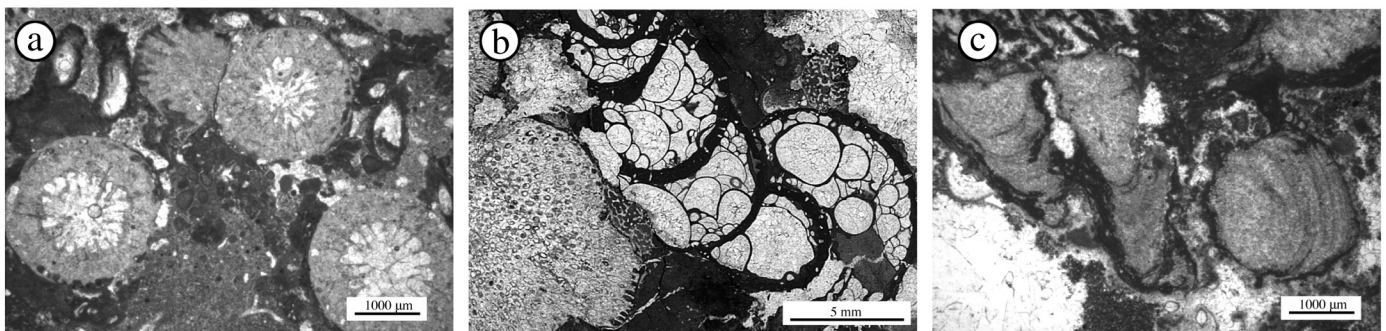


Fig. 6. Transmitted light microphotographs of Alpe di Specie samples: a) *Margarosmia* sp., sample S1; b) *Colospongia andrusovi*, sample S2; c) 'Solenopora', sample S.



Fig. 7. Scleractinian, red algal, sponge, bryozoan frame reef macrofabrics, Alpedi Specie. a) Large corals at center and left are *Margarosmilia*. b) Sample dominated by the inozoan sponge *Sestrostomella robusta*.

They show strong predominance of hexa- and octadecanoic acids (C_{16} , C_{18}) and small amounts of high molecular weight compounds in the region from C_{23} to C_{27} . Terminally-branched fatty acids are absent from the lipid fractions of Punta Grohmann samples (Fig. 10a).

The m/z 57 + 71 + 85 + 99 + 113 mass fragmentogram of the aliphatic hydrocarbon fraction extracted from Punta Grohmann samples shows a wide variety of branched and unbranched long chain n-alkanes and the presence of specific acyclic isoprenoid compounds, recognized as pristane and phytane. The average pristane/phytane ratio (Pr/Ph) is >1 ; this suggests oxygenated conditions during deposition (see Rashid, 1979; Powell, 1988).

GC-MS analyses of all the samples studied reveal extended hopane series from C_{27} to C_{31} , but these are more abundant in the Punta Grohmann samples. The partial m/z 191 mass fragmentogram of the hydrocarbons provides evidence of hopanoid distributions. Both $\alpha\beta$ and $\beta\alpha$ isomers are present for most of the compounds. The hopanoid distribution is dominated by non-extended hopanes; predominantly the C_{30} member ($17\alpha,21\beta$ -hopane). The other compounds include C_{29} ($17\alpha,21\beta$ -norhopane), C_{27} (17β and 17α -trisorhopane), C_{29} ($17\beta,21\alpha$ and $17\beta,21\beta$ -norhopane), C_{30} ($17\beta,21\beta$ -hopane), C_{31} ($17\alpha,21\beta$ and $17\beta,21\alpha$ -homohopane) and C_{32} ($17\alpha,21\beta$ -bisomohopane). The carboxylic acid pattern and pentacyclic terpanes series in the Punta Grohmann samples are similar to those reported from present-day microbial mats in the Florida Everglades, indicating an origin from calcifying cyanobacteria (see Thiel et al., 1997). However,

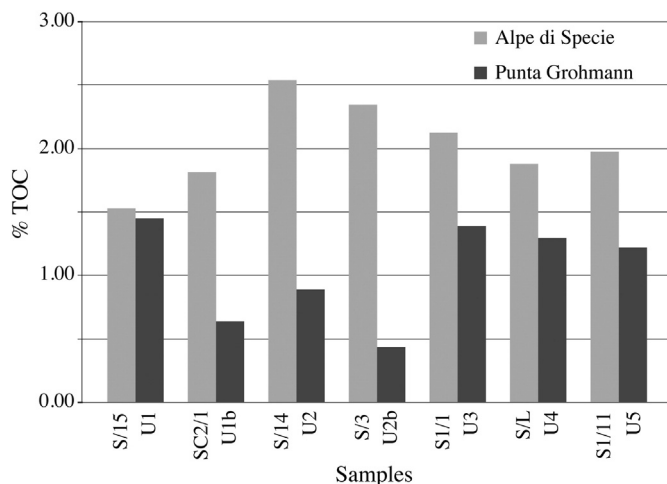


Fig. 8. Total Organic Carbon (TOC) content of samples from Punta Grohmann and Alpe di Specie.

monounsaturated fatty acids, as well as saturated short-chain fatty acids, have low specificity, occurring in a variety of marine bacteria (Cranwell, 1982; Parkes and Taylor, 1983; Gillan and Sandstrom, 1985), marine phytoplankton (e.g., Volkmann et al., 1989; Viso and Marty, 1993; Pond et al., 1998), zooplankton, and benthic organisms (e.g., Wakeham, 1995; Albers et al., 1996; Graeve et al., 1997). The presence of hopanoids, although not abundant, also indicates prokaryotes (Ourisson et al., 1987; Brocks and Summons, 2003). Studies have shown that pentacycliterpanes of the C_{27} to C_{31} hopane series are diagnostic of bacteria (Brocks and Summons, 2003; Peters et al., 2005a, 2005b). Bacteriohopanepolyols, the biological precursors of these hopanes, have function as membrane rigidifiers in bacteria, the equivalent role to that performed in Eukarya by sterols (Ourisson et al., 1987; Brocks and Summons, 2003).

In Alpe di Specie samples, C_{16} monounsaturated and C_{18} mono- and diunsaturated compounds are present in significant amounts in the peloidal microfabric (Fig. 10b). These also contain terminally-branched $C_{15:0}$ to $C_{19:0}$ *iso* and *anteiso* fatty acids. Among the *iso* and *anteiso* fatty acids, those with 15 and 17 carbons are more abundant. *Iso* fatty acids predominate over *anteiso* fatty acids. Short-chain

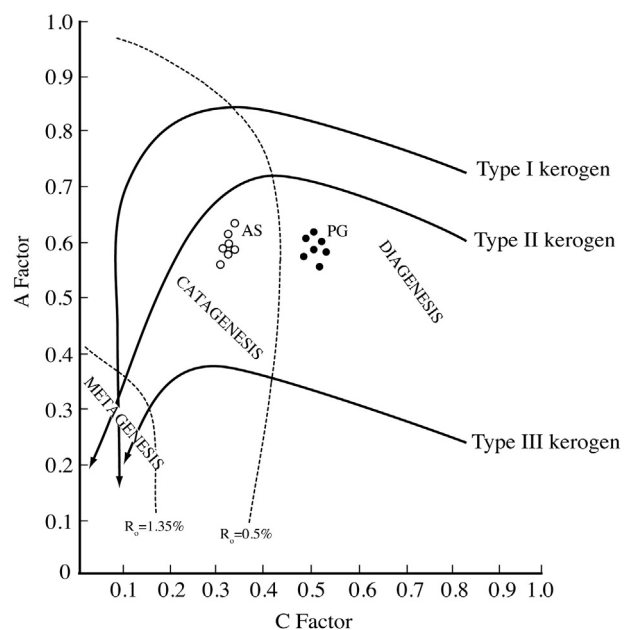


Fig. 9. Van Krevelen diagram showing thermal maturity of samples from Punta Grohmann (PG, filled circles) and Alpe di Specie (AS, open circles).

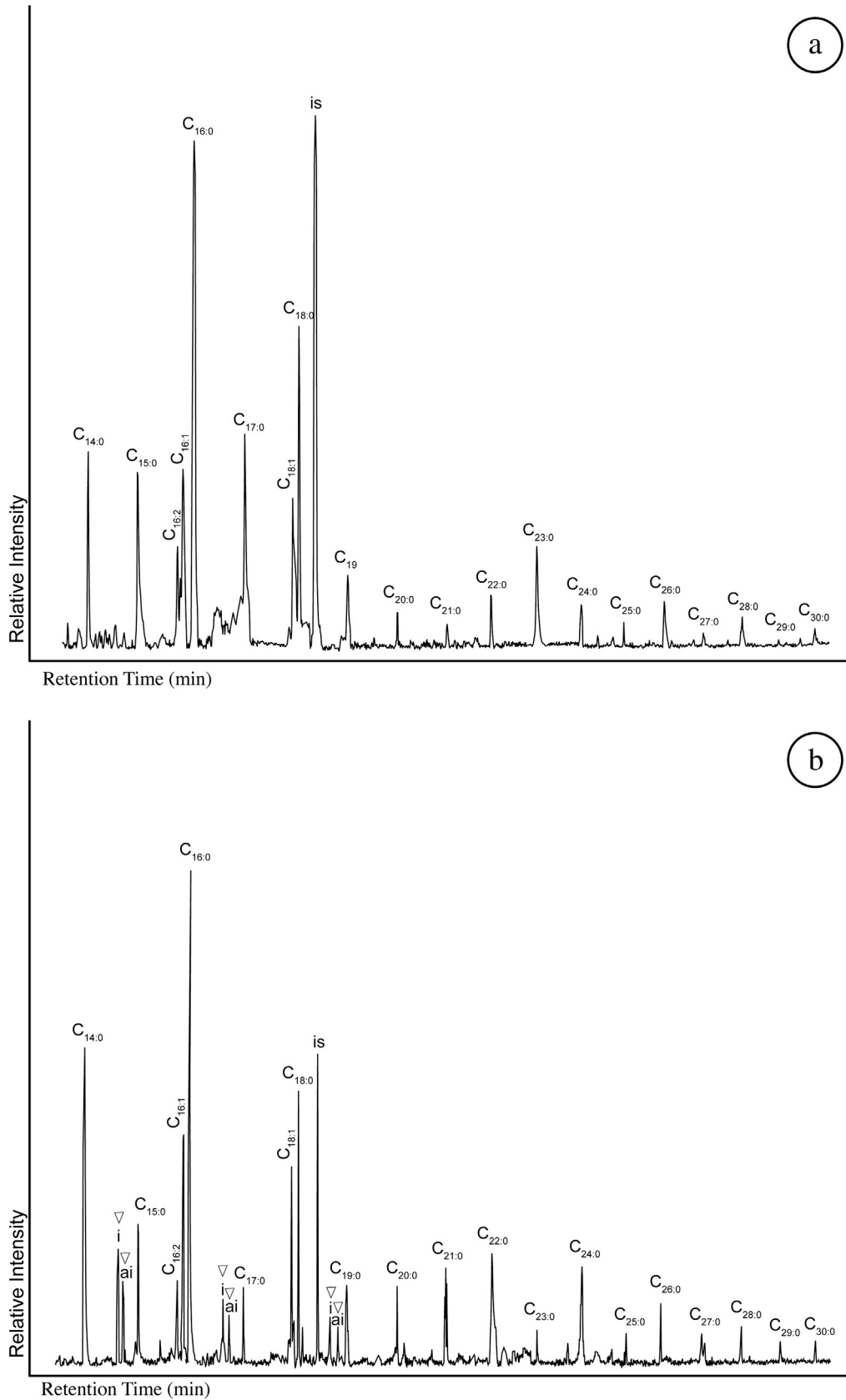


Fig. 10. Partial gas chromatogram of the acidic fraction showing distribution of fatty acids: a) Punta Grohmann; b) Alpe di Specie.

branched fatty acids occur in various bacteria (e.g., Edlund et al., 1985; Goossens et al., 1986; Kaneda, 1991), but *iso*- and *anteiso*-C_{15:0} and C_{17:0}-branched fatty acids are particularly abundant in sulfate-

reducers (Perry et al., 1979; Taylor and Parkes, 1983; Dowling et al., 1986; Wakeham and Beier, 1991; Elvert et al., 2003; Heindel et al., 2010, 2012; Guido et al., 2013c). Since cyanobacteria are not known to

Table 1
REE + Y concentrations (in ppm) in samples from Punta Grohmann and Alpe di Specie. Calculations of the La, Ce, anomalies, Y/Ho and Sm_{sn}/Yb_{sn} ratios for the samples, and the certified and measured values of the standards (NIST Argillaceous Limestone, SRM1d, and USGS Micaschist, SDC-1), are also shown.

	Samples																
	UIA	UZS	U2M	U3	U4	U5	S	S1	S1-1	S3	SL	SC2-1	PAAS (standard)	SDC-1 certified value	SDC-1 measured value	SRM1d certified value	SRM1d measured value
Sc	0.72	0.97	0.39	0.71	0.89	0.92	0.84	0.99	0.96	0.59	0.46	0.75	-	17.00	23.13	-	3.68
La	1.11	4.39	5.99	2.65	4.68	0.85	0.38	1.91	1.87	1.11	2.29	0.31	38.20	-	51.70	5.00	5.52
Ce	1.19	6.05	6.69	3.42	6.85	0.80	0.61	3.58	4.81	2.53	5.57	0.56	79.60	39.00	40.15	4.00	3.02
Pr	0.20	1.00	1.41	0.56	1.14	0.14	0.06	0.37	0.56	0.27	0.86	0.05	8.83	93.00	91.60	4.00	3.91
Nd	0.98	4.20	7.42	2.71	5.42	1.02	0.30	1.93	2.91	1.38	4.71	0.31	33.90	-	8.07	0.60	0.47
Sm	0.19	0.82	1.46	0.53	1.07	0.14	0.05	0.39	0.61	0.27	0.99	0.04	5.55	40.00	42.66	3.00	2.40
Eu	0.05	0.22	0.40	0.15	0.30	0.04	0.02	0.11	0.16	0.07	0.25	0.02	1.08	8.50	8.56	0.50	0.46
Gd	0.26	0.98	1.78	0.72	1.36	0.18	0.07	0.48	0.76	0.31	1.15	0.08	4.66	1.70	1.85	0.10	0.11
Tb	0.04	0.13	0.24	0.10	0.19	0.03	0.01	0.07	0.11	0.04	0.16	0.01	0.77	7.40	8.81	0.50	0.57
Dy	0.24	0.79	1.40	0.64	1.12	0.17	0.06	0.43	0.70	0.27	0.98	0.07	4.68	1.20	1.29	0.09	0.08
Y	3.92	9.32	15.39	9.72	11.61	2.62	0.73	3.92	5.94	2.03	7.02	0.68	27.00	6.70	7.38	0.60	0.52
Ho	0.06	0.16	0.28	0.15	0.23	0.04	0.02	0.09	0.15	0.05	0.19	0.02	0.99	1.50	1.47	0.10	0.11
Er	0.18	0.46	0.85	0.46	0.69	0.12	0.04	0.28	0.45	0.16	0.58	0.05	2.85	4.10	4.39	0.40	0.32
Tm	0.03	0.06	0.11	0.07	0.09	0.02	0.01	0.04	0.06	0.02	0.08	0.01	0.41	0.65	0.63	-	0.04
Yb	0.18	0.45	0.77	0.38	0.71	0.11	0.03	0.20	0.35	0.13	0.48	0.04	2.82	4.00	4.02	0.30	0.27
Lu	0.03	0.07	0.12	0.07	0.09	0.02	0.01	0.04	0.06	0.02	0.08	0.01	0.43	-	0.62	-	0.04
Th	0.11	0.50	0.27	0.19	0.23	0.06	0.05	0.20	0.29	0.17	0.69	0.72	-	11.10	10.72	-	0.40
(La/La*) _{sn}	2.33	2.15	1.77	2.19	2.02	0.51	1.41	3.09	3.81	1.62	3.27	0.67	-	-	-	-	-
(Ce/Ce*) _{sn}	0.83	0.99	0.64	0.90	0.92	0.26	1.00	1.51	1.63	1.25	1.19	0.64	-	-	-	-	-
Y/Ho	65.67	58.75	55.23	65.64	50.79	67.16	46.69	42.43	40.26	38.06	36.33	37.84	-	-	-	-	-
Sm_{sn}/Yb_{sn}	0.55	0.92	0.96	0.71	0.77	0.64	0.87	1.01	0.88	1.03	1.06	0.57	-	-	-	-	-

synthesize *iso*- and *anteiso*-branched fatty acids with chain lengths C₁₅ and C₁₇, it is reasonable to interpret these short-chain branched fatty acids as biomarkers for sulfate reducers with intermediate source specificity (Heindel et al., 2010, 2012). The relative abundance of these biomarkers suggests that the bacterial community was dominated by sulfate-reducing bacteria. By degrading reefal organic matter, as in present-day autochthonous reef crusts, SRB appear to induce precipitation of clotted peloidal micrite deposits in reef frameworks (Heindel et al., 2010, 2012; Guido et al., 2013c).

4.4. Rare Earth Elements

REE + Y values of the samples studied, with calculated anomalies and control standards values, are shown in Table 1. Punta Grohmann REE distributions, normalized to PAAS (PostArchean Australian Shales; Nance and Taylor, 1976; Webb and Kamber, 2000), show coherent patterns, with positive La, negative Ce, and a subordinate negative Pr anomaly (Fig. 11). The average La and Ce anomalies are 1.83 ± 0.67 and 0.75 ± 0.27 respectively (Table 1). These values also show relative depletion in lighter rare earths (LREE) and low enrichment of the heavy rare earths (HREE), expressed by the average value ratios of Sm_{sn}/Yb_{sn} (ratio = 0.76; SD = 0.16) according to Webb and Kamber (2000). The samples also show a strongly superchondritic Y/Ho ratio, expressed as a prominent positive Y spike in the pattern (Y/Ho = 60.54, SD = 6.67), corresponding with the range of modern marine proxies (44–74) (Nozaki et al., 1997) and considerably higher than chondritic values (26–28) (Kamber and Webb, 2001). Cerium values can be interpreted as a function of the oxidation state (Elderfield and Greaves, 1982; Webb and Kamber, 2000; Bolhar et al., 2004). The Punta Grohmann Ce values indicate deposition in normal oxygenated conditions. They are similar to those in Lower and Upper Permian bioclastic limestones in China (Nan Junya et al., 2002) which are characterized by relative HREE enrichment, considerable Ce depletion, and positive La. Modern microbialites possess a prominent negative Ce anomaly, $(Ce/Ce^*)_{sn} < 1$, and a positive La anomaly, $(La/La^*)_{sn} > 1$ (Webb and Kamber, 2000).

Alpe di Specie REE distributions, PAAS normalized, show a flatter pattern than those at Punta Grohmann, with positive La and Ce anomalies, a negative Pr anomaly, and a reduced Y spike (Fig. 10). The samples exhibit lower HREE enrichment (Sm_{sn}/Yb_{sn} ratio = 0.90; SD = 0.18). Average La and Ce anomalies are 2.31 ± 1.25 and 1.20 ± 0.36 respectively (Table 1). The Ce anomaly is coherent with sub-oxic deposition (Nan Junya et al., 2002). These values can also be compared with those in blocks of Jurassic marine limestones in Japan, interpreted as having been deposited in a restricted environment in which local waters were more reducing than normal (Tanaka et al., 2003). Other examples with similar values can be found in present-day stagnant water masses, as in anoxic waters of the Cariaco Trench (De Baar et al., 1988). The Y/Ho ratio is interpreted as near chondritic (sample average Y/Ho ratio is 40.27 ± 3.80) and is consistent with limited terrigenous influx indicated by lower concentration of Sc and Th (Bau and Dulski, 1996; Van Kranendonk et al., 2007; Table 1). The overall REE distributions in Alpe di Specie samples, showing negative Pr and lower positive Y anomalies with a chondritic-type Y/Ho ratio, suggest less oxygenated depositional conditions (Webb and Kamber, 2000; Bolhar et al., 2004) than those in Punta Grohmann samples.

5. Discussion

Flügel (2002, Table 1) recognized three main stages of Triassic reef development: Scythian microbial reefs, Anisian–Carnian sponge–*Shamovella*–microbial crust reefs, and Norian–Rhaetian sponge–coral–red algal reefs. In the Dolomite region the key step, when the sponge–*Shamovella*–crust reef biota was augmented by corals and calcareous algae, occurred within the second of these stages, near the Ladinian–Carnian transition (Flügel, 2002; Stanley, 2003; Russo, 2005), and coincided with an apparent reduction in the rate of carbonate sedimentation, or at

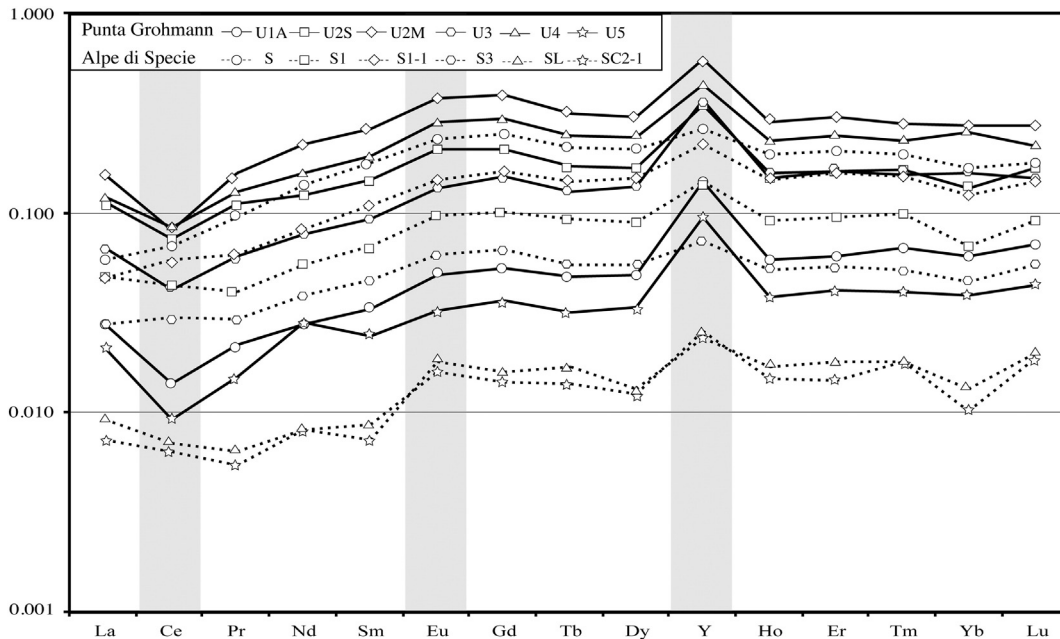


Fig. 11. REE distribution patterns, normalized to PAAS (McLennan, 1989), of the samples from Punta Grohmann and Alpe di Specie. Punta Grohmann samples are characterized overall by positive La and negative Ce anomalies, an HREE enriched pattern, the presence of Gd and Eu anomalies, and a high Y spike. Alpe di Specie samples show a flatter distribution, with lower Ce and Y anomalies and a prominent negative Pr anomaly, suggesting a less oxygenated environment.

least a decline in the formation of high-rise prograding platforms (Keim et al., 2006). Current age estimates for the base of the Ladinian (241.5 Ma) and the base of the Carnian (237 Ma) (Gradstein et al., 2012), are respectively ~4.5 Ma and ~9 Ma older than previously calculated (Ogg et al., 2008), and indicate that these significant Ladinian–Carnian changes in reef composition took place within ~15 Ma of the Permian–Triassic boundary.

5.1. Punta Grohmann microbial-problematica-sponge reef

Despite the major changes in environments and organisms associated with the Permian–Triassic Mass Extinction transition (Erwin, 2006; Knoll et al., 2007), the reef building communities that dominated the Ladinian in the Dolomites show similarities to those of the mid–late Permian. They were dominated by heavily calcified but mostly very small skeletons, locally in close association with large amounts of syndeositional cemented micrite, microbial veneers, and small fenestrate (Fürsich and Wendt, 1977; Russo et al., 1997). Their microfacies are broadly similar to those of the Late Permian Capitan reef (Stanley, 1981, 1988; Wood, 1998). Punta Grohmann reefs include bryozoans, calcified cyanobacteria (*Cladogirvanella*, *Girvanella*), and sponges together with diverse problematic calcified organisms (e.g. *Shamovella*), microbial crusts (e.g., *Archaeolithoporella*), sparry seafloor crusts and abundant micrite, much of which has been regarded as microbial in origin. These small heavily calcified organisms, connected by syndeositionally lithified autochthonous micrites and crusts, built a structure well suited to high energy conditions (Russo et al., 1997). There is little evidence that coarse-grained allochthonous debris accumulated in this environment. Similar reef architecture, forming wave-resistant platform margins and slopes have been observed in Zechstein reefs of northern England (Tucker and Hollingworth, 1986), the Permian Capitan Reef of west Texas and New Mexico (Wood et al., 1994, 1996) and in Triassic megablocks in Sosio Valley, Sicily (Flügel et al., 1991).

In Punta Grohmann samples, the REE + Y pattern and pristane/phytane ratio (>1) indicate an aerobic environment, and the fatty acid distribution and presence of hopanoids indicate cyanobacteria (Tosti et al., 2011b, 2012). Oxygenation is consistent with the high-energy environment of this exposed reef margin location, and cyanobacterial

biomarkers are consistent with the common presence of *Girvanella* and *Cladogirvanella* in the samples. The absence of BSR biomarkers suggests that these tight structures created few cavities in which low-oxygen conditions could develop. It had previously been assumed that the abundant micrite in Punta Grohmann reefs likely had a microbial origin similar to that inferred for Alpe di Specie (Russo et al., 1991; Tosti et al., 2012). However, in the light of our biomarker data, it is necessary to revisit the question of the nature and origin of the abundant micrite in reefs of Punta Grohmann type.

5.2. Alpe di Specie corallgal frame reef

Large, extensive metazoan reefs with corals became common in the Upper Triassic, primarily in the Tethys and western Panthalassa oceans (Flügel, 2002; Martindale et al., 2010). By comparison, Alpe di Specie patch-reefs are small. They are similar to Carnian patch reefs from Williston Lake (British Columbia, Canada) described by Zonneveld et al. (2007) which have metric dimensions and are mainly composed of scleractinian corals, sponges and red algae with the additional presence of green algae, bryozoans and problematic microorganisms. Micrites, filling the cavities, can present a distinctive clotted fabric (Patch-Reef B and C; Zonneveld et al., 2007).

REE + Y signatures and abundance of organic matter in Alpe di Specie samples indicate suboxic environments. Neuweiler and Reitner (1995) found bright fluorescence associated with growth forms of thrombolites and stromatolites in polished thin-sections. They interpreted this to indicate in situ organic matter and to be organomicrite. We infer that these deposits preferentially developed in reefal cavities, favored by proliferation of essentially anaerobic bacterial communities such as those indicated by the presence of BSR biomarkers. This new finding supports but also qualifies Keim et al's (2006) suggestion of anoxic conditions. We infer that this reef community required at least ~3 to 5 ml·l⁻¹ of dissolved oxygen (Neulinger et al., 2008) mainly produced by algae. Furthermore, the sub-oxic conditions indicated by REE may reflect local microenvironments within the reef cavities that were different from the oxygen levels of the surface seawater. BSR biomarkers are consistent with suboxic conditions generally, because sulfate reduction typically occurs in oxygen-poor environments, and with the development of restricted cavities in

which organic matter could accumulate and decay. The clotted peloidal micrite within these types of framework cavities has commonly been linked to anaerobic bacteria (Monty, 1976; Chafetz, 1986; Buczynski and Chafetz, 1991; Reitner, 1993; Kazmierczak et al., 1996; Folk and Chafetz, 2000; Riding, 2002; Riding and Tomás, 2006) and comparable fabrics in Pleistocene–Holocene reef microbialites at Tahiti contain lipid biomarkers indicating a bacterial community dominated by sulfate-reducing bacteria that degraded organic matter (Heindel et al., 2010, 2012). Similarly, Guido et al. (2012c, 2013c) recognized the involvement of SRB in micrite precipitation in Holocene biostalactites in submerged caves in Sicily.

5.3. Cyanobacterial calcification

Cladogirvanella is an unusually large and well-calcified cyanobacterial fossil that in Punta Grohmann reef fabrics forms centimetric erect dendritic skeletons (Ott, 1966; Russo et al., 1997). Modeled results suggest that, following the Permian–Triassic transition, atmospheric CO₂ declined to relatively low levels ~220 Ma ago (Berner, 2006, Fig. 18) as O₂ levels increased (Berner, 2006, Fig. 20). These conditions can be expected to induce CO₂ concentrating mechanisms (CCM) in cyanobacteria. CCM act to maintain photosynthesis, and include bicarbonate transport into cells (Badger and Price, 2003). This in turn promotes extracellular pH rise that can cause sheath calcification if aquatic carbonate saturation state is elevated (Merz, 1992; Riding and Tomás, 2006). A modeled increase in seawater calcium levels at this time (Stanley and Hardie, 1998, Fig. 1) suggests that seawater saturation for CaCO₃ minerals would also have increased (Riding and Liang, 2005a), consistent with high accumulation rates of platform carbonates at this time (Bosscher and Schlager, 1993) (see Riding and Liang, 2005b, Fig. 1), as is well seen in the Italian Dolomites. It is therefore possible that Triassic increase in occurrence of marine sheath-calcified cyanobacteria (Arp et al., 2001, Fig. 1d) reflects this combination of conditions. These inferences are consistent with expectations that Permian–Triassic biotic changes reflect responses to major environmental perturbations, that probably influenced both abiotic and bioinduced CaCO₃ precipitation (Goddéris et al., 2008; Kiessling, 2010).

5.4. Reef cavity anoxia

Cavernous reef frameworks are important in increasing habitat diversity and providing sites for both the production and mineralization of organic matter (Haberstroh and Sansone, 1999; Richter et al., 2001).

These processes can significantly influence early diagenesis (Zankl and Müller, 1977) and nutrient regeneration and cycling (Werner et al., 2006). Not least, they may have assisted coral reefs to occupy oligotrophic oceanic conditions (Crossland and Barnes, 1983; Werner et al., 2006). Frameworks have developed in many Phanerozoic skeletal reefs (Webb, 1996; Riding, 2002), but cavities are likely to have been smaller where constructors were laminar skeletons and where matrix and/or intense syndepositionary cementation and surface crusts rapidly occluded pores and internal space. As in the Latemar margin reef (Harris, 1993), reef structure in the Punta Grohmann samples was cavity-poor and dominated by small and often encrusting skeletons (Fürsich and Wendt, 1977; Biddle, 1981; Russo et al., 1997). The development of Alpe di Specie reefs appears to have marked a reversion to more open frame-reef structure. Certainly, by the Late Triassic scleractinian corals were becoming major reef builders (Flügel, 1994), locally developing substantial frameworks (Weidlich et al., 1993; Bernecker, 2005).

6. Synthesis and conclusions

Punta Grohmann and Alpe di Specie reef carbonates represent a significant transition in reef construction and environments. Excellent preservation and low thermal maturity allow detailed organic compound characterization to be combined with REE analyses and petrographic characteristics, providing an integrated interpretation of these deposits (Fig. 12).

Punta Grohmann carbonates are generally well preserved erratic blocks (Cipit Boulders), embedded in marly matrix and derived from adjacent prograding carbonate platforms. They are widely thought to represent rigid reef framework that developed in shallow-water on platform margins or upper slopes (Keim and Schlager, 2001). Their fabrics contain calcified cyanobacteria, problematic organisms (*Archaeolithoporella*, *Shamovella*), and sponges together with locally large amounts of syndepositionally cemented micrite, and sparry seafloor crust. Together, these created reef structures with few large cavities. REE values indicative of oxic conditions are consistent with this setting and reef structure. Although the absence of specific biomarkers for BSR does not necessarily imply that sulfate reduction did not occur, it suggests that most organic matter was likely efficiently removed by aerobic processes. Distinct biomarkers for cyanobacteria are consistent with the presence of common calcified cyanobacterial fossils in these frameworks. These results support the widely held view that microbial processes were involved in forming these deposits, but at the same time indicate a stronger connection with cyanobacterial oxygenic photosynthesis than with BSR. This underscores

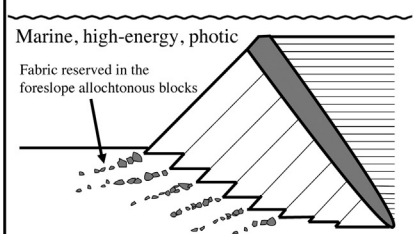
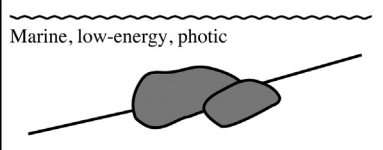
	Ladinian-Carnian, Punta Grohmann	Carnian, Alpe di Specie
	Elevated platform margin reef	Ramp patch reef
		
Fabric	sponge-microbial-problematica sea-floor crust reef	coral-sponge, red algal cement-poor frame reef
Microbial carbonate	cyanobacteria, biofilm, peloid micrite	peloid micrite
TOC Content	lower	higher
Organic Matter Preservation	good	very good
Biomarkers	cyanobacteria	sulfate reducers
REE interpretation	oxic	sub-oxic

Fig. 12. Summary details of contrasting reef carbonates preserved in mid-Triassic allochthonous blocks of reef margin from Punta Grohmann and in Alpe di Specie patch reefs.

a need to further examine the origins of the micritic fabrics that are common in these platform-top deposits (Russo et al., 1997; Stefani et al., 2004). Oxidic conditions are consistent with warm turbulent shallow-water, which is likely to have an elevated carbonate saturation state. This, together with mid-Triassic conditions (more elevated oxygen; lower levels of CO₂) that promote induction of CO₂-concentrating mechanisms could have combined to stimulate bioinduced cyanobacterial calcification, accounting for the unusual abundance of these fossils at this time (see Arp et al., 2001).

Alpe di Specie patch reefs formed in quieter shallow water environments that were muddy but photic. Their relatively open and cavernous framework was constructed mainly by scleractinian corals, sponges, and red algae. Seafloor sparry crusts are lacking and distinctive clotted-peloidal micrite fabrics accumulated in relatively large cavities. Despite their small size, these Carnian (~234 Ma) bioherms constitute one of the earliest examples of skeletal framework biotically similar to that of present-day tropical coral reefs, composed mainly of scleractinian corals and coralline algae. This framework favored the formation of cavities with clotted-peloidal microbial carbonate fabrics. Lipid biomarkers indicate that the bacterial community was dominated by BSR, which presumably degraded dissolved and particulate organic matter derived from within the reef. Low energy conditions coupled with enclosed cavity development therefore promoted cryptic suboxic environments, as reflected by REE values and consistent with the presence of biomarkers for sulfate reducers. Despite the large difference in age and reef dimensions, these conditions and microbial processes resemble those of some Late Pleistocene–Early Holocene coral reefs, with BSR-dominated cryptic communities that form stromatolitic crusts.

Ladinian–Carnian reefs in the Dolomites therefore reflect evolution from Permian-like reef constructions, with abundant crusts and autochthonous microbial synsedimentary lithification, to more open cavernous scleractinian–red algal frameworks that anticipate essential features of much younger reefs. Redox geochemistry and biogeochemistry closely reflect the combined effects that framework structure and extrinsic environmental factors produced on internal organic carbon cycling in these mid-Triassic reefs.

Acknowledgments

We thank Attilio Naccarato and Antonio Tagarelli for their help with the analytical procedures. We greatly appreciate the suggestions of two anonymous reviewers and the editorial advice of David Bottjer that improved the final version.

References

- Albers, C.S., Kattner, G., Hagen, W., 1996. The compositions of wax esters, triacylglycerols and phospholipids in Arctic and Antarctic copepods: evidence of energetic adaptations. *Mar. Chem.* 55, 347–358.
- Arp, G., Reimer, A., Reitner, J., 2001. Photosynthesis-induced biofilm calcification and calcium concentrations in Phanerozoic oceans. *Science* 292, 1701–1704.
- Assereto, R., Brusca, C., Gaetani, M., Jadoul, F., 1977. The Pb–Zn mineralization in the Triassic of the Dolomites. Geological history and genetic interpretation. *Ind. Mineraria* 28, 267–302 (Roma).
- Badger, M., Price, D., 2003. CO₂ concentrating mechanisms in cyanobacteria: molecular components, their diversity and evolution. *J. Exp. Bot.* 54, 609–622.
- Baranger, P., Disnar, J.R., 1988. Non-aromatic biomarkers associated with a Paleogene salt formation (Bresse, France). *Org. Geochem.* 13, 647–653.
- Baranger, P., Disnar, J.R., Farjanel, G., Fourmont, P., 1989. Confrontation de données géochimiques et optiques quantitatives et qualitatives sur la matière organique associée aux séries salifères de Bresse. *Bull. Soc. Géol. France* 8, 967–978.
- Bartle, K.D., Jones, D.W., Pakdel, H., Snape, C.E., Calimli, A., Olcay, A., Tügrü, T., 1979. Paraffinic hydrocarbons from supercritical gas extracts of coal as organic geochemical tracers. *Nature* 277, 285–287.
- Bau, M., Dulski, P., 1996. Distribution of yttrium and rare-earth elements in the Penge and Kuruman iron-formations, Transvaal Supergroup, South Africa. *Precambrian Res.* 79, 37–55.
- Bernasconi, S.M., Riva, A., 1993. Organic geochemistry and depositional environment of a hydrocarbon source rock: the Middle Triassic Grenzbitumenzone Formation, Southern Alps, Italy/Switzerland. In: Spencer, A.M. (Ed.), *Generation, Accumulation and Production of Europe's Hydrocarbons III*. Special Publication of the European Association of Petroleum Geologists, 3. Springer, Heidelberg, pp. 179–190.
- Bernecker, M., 2005. Late Triassic reefs from the Northwest and South Tethys: distribution, setting, and biotic composition. *Facies* 51, 442–453.
- Berner, R.A., 2006. GEOCARBSULF: a combined model for Phanerozoic atmospheric O₂ and CO₂. *Geochim. Cosmochim. Acta* 70 (23), 5653–5664.
- Biddle, K.T., 1981. The basinal Cipit boulders: indicators of Middle to Upper Triassic buildup margins, Dolomite Alps, Italy. *Riv. Ital. Paleontol. Stratigr.* 86, 779–794.
- Bolhar, R., Kamber, B.S., Moorbath, S., Fedo, C.M., Whitehouse, M.J., 2004. Characterisation of early Archaean chemical sediments by trace element signatures. *Earth Planet. Sci. Lett.* 222, 43–60.
- Bosellini, A., 1984. Progradation geometries of carbonate platforms: example from the Triassic of the Dolomites (northern Italy). *Sedimentology* 31, 1–24.
- Bosellini, A., Rossi, D., 1974. Triassic carbonate buildups of the Dolomites, northern Italy. In: Laporte, L.F. (Ed.), *Reefs in Time and Space*. Spec. Publ. Soc. Econ. Paleont. Miner., Tulsa, 18, pp. 209–233.
- Bosscher, H., Schlager, W., 1993. Accumulation rates of carbonate platforms. *J. Geol.* 101, 345–355.
- Brandner, R., Burger, U., Gögl, M.L., Gruber, A., Gruber, J., Jesacher, M., Keim, L., Pirchl, T., Prager, C., Psenner, A., Schmid, M., 2007. Geologische Karte der Westlichen Dolomiten, West-Blatt, Ost-Blatt und Profilschnitte, 1:25.000. Amt für Geologie und Baustoffprüfung, Autonome Provinz Bozen.
- Brocks, J.J., Summons, R.E., 2003. Sedimentary hydrocarbons, biomarkers for early life. In: Schlesinger, W.H. (Ed.), *Treatise on Geochemistry. Biogeochemistry, Vol 8*. Elsevier-Perгамon, Oxford, pp. 63–115.
- Buczynski, C., Chafetz, H.S., 1991. Habit of bacterially induced precipitates of calcium carbonate and the influence of medium viscosity on mineralogy. *J. Sediment. Petrol.* 61, 226–233.
- Chafetz, H.S., 1986. Marine peloids, a product of bacterially induced precipitation of calcite. *J. Sediment. Petrol.* 56, 812–817.
- Cranwell, P.A., 1982. Lipids of aquatic sediments and sedimenting particulates. *Prog. Lipid Res.* 21, 271–308.
- Crossland, C.J., Barnes, D.J., 1983. Dissolved nutrients and organic particulates in water flowing over coral reefs at Lizard-Island. *Aust. J. Mar. Freshw. Res.* 34, 835–844.
- Cuif, J.P., Gautret, P., Laghi, G.F., Mastandrea, A., Pradier, B., Russo, F., 1990. Recherche sur la fluorescence UV du squelette apicalaire chez les Démospanges calcitiques triasiques. *Geobios* 23, 21–31.
- De Baar, H.J.W., German, C.R., Elderfield, H., Van Gaans, P., 1988. Rare earth element distributions in anoxic waters of the Cariaco Trench. *Geochim. Cosmochim. Acta* 52, 1203–1219.
- De Zanche, V., Gianolla, P., Mietto, P., Siorpaes, C., Vail, P.R., 1993. Triassic sequence stratigraphy in the Dolomites (Italy). *Mem. Sci. Geol.* 45, 1–27.
- De Zanche, V., Gianolla, P., Roghi, G., 2000. Carnian stratigraphy in the Raibl/Cave del Predil area (Julian Alps, Italy). *Ecol. Geol. Helv.* 93, 331–347.
- Dieci, G., Antonacci, A., Zardini, R., 1970. Le spugne cassiane (Trias medio-superiore) della regione dolomitica attorno a Cortina d'Ampezzo. *Boll. Soc. Paleontol. Ital.* 7, 94–155.
- Dowling, N.J.E., Widdel, F., White, D.C., 1986. Phospholipid ester-linked fatty acid biomarkers of acetate-oxidizing sulphate-reducers and other sulphide-forming bacteria. *J. Gen. Microbiol.* 132, 1815–1825.
- Edlund, A., Nichols, P.D., Roffky, R., White, D.C., 1985. Extractable and lipopolysaccharide fatty acid and hydroxy acid profiles from *Desulfovibrio* species. *J. Lipid Res.* 29, 982–988.
- Eggins, S.M., Woodhead, J.D., Kinsley, L.P.J., Mortimer, G.E., Sylvester, P., McCulloch, M.T., Hergt, J.M., Handler, M.R., 1997. A simple method for the precise determination of ≥ 40 trace elements in geological samples by ICPMS using enriched isotope internal standardisation. *Chem. Geol.* 134, 311–326.
- Elderfield, H., Greaves, M.J., 1982. The rare earth elements in seawater. *Nature* 296, 214–219.
- Elvert, M., Boetius, A., Knittel, K., Jørgensen, B.B., 2003. Characterization of specific membrane fatty acids as chemotaxonomic markers for sulfate-reducing bacteria involved in anaerobic oxidation of methane. *Geomicrobiol. J.* 20, 403–419.
- Erwin, D.H., 2006. *Extinction: How Life on Earth Nearly Ended 250 Million Years Ago*. Princeton University Press, Princeton, NJ.
- Flügel, E., 1994. Pangean shelf carbonates: controls and paleoclimatic significance of Permian and Triassic reefs. *Geol. Soc. Am. Spec. Pap.* 288, 247–266.
- Flügel, E., 2002. Triassic reef patterns. In: Kiessling, W., Flügel, E., Golonka, J. (Eds.), *Phanerozoic Reef Patterns*. SEPM Special Publication, 72, pp. 391–463 (Tulsa).
- Flügel, E., Stanley, G.D., 1984. Reorganisation, development and evolution of post-Permian reefs and reef organisms. *Palaeontogr. Am.* 54, 177–186.
- Flügel, E., Di Stefano, P., Senowbari-Daryan, B., 1991. Microfacies and depositional structure of allochthonous carbonate base-of-slope deposits: the late Permian Pietra di Salomone megablock, Sosio Valley (Western Sicily). *Facies* 25, 147–186.
- Folk, R.L., Chafetz, H.S., 2000. Bacterially induced microscale and nanoscale carbonate precipitates. In: Riding, R.E., Awramik, S.M. (Eds.), *Microbial Sediments*. Springer Verlag, Berlin, pp. 40–49.
- Fürsich, F.T., Wendt, J., 1977. Biostratigraphy and palaeoecology of the Cassian Formation (Triassic) of the Southern Alps. *Palaeogeogr. Palaeoclimatol. Palaeoecol.* 22, 257–323.
- Gaetani, M., Fois, E., Jaoul, F., Nicora, A., 1981. Nature and evolution of middle Triassic carbonate buildups in the Dolomites (Italy). *Mar. Geol.* 44, 25–57.
- Ganz, H., Kalkreuth, W., 1987. Application of infrared spectroscopy to the classification of kerogen-types and the evolution of source rock and oil shale potentials. *Fuel* 66, 708–711.
- Gianolla, P., Neri, C., 2007. Formazione di Wengen. In: Cita Sironi, M.B., Abbate, E., Balini, M., Conti, M.A., Falorni, P., Germani, D., Gropelli, G., Manetti, P., Petti, F.M. (Eds.), *Carta Geologica d'Italia 1:50.000, Catalogo delle Formazioni – Unità tradizionali (2)*, QUADERNI serie III, 7/VIII. S.E.L.C.A., Firenze, pp. 111–124.

- Gianolla, P., De Zanche, V., Mietto, P., 1998. Triassic sequence stratigraphy in the Southern Alps. Definition of sequences and basin evolution. In: de Graciansky, P.C., Hardenbol, J., Jacquin, T., Vail, P.R., Ulmer-Scholle, D. (Eds.), *Mesozoic–Cenozoic Sequence Stratigraphy of European Basins*. SEPM Special Publication, 60, pp. 723–751.
- Gianolla, P., Avanzini, M., Breda, A., Kustatscher, E., Preto, N., Roghi, G., Furin, S., Massari, F., Picotti, V., Stefani, M., 2010. Dolomites. 7th International Triassic Workshop Field Guide.
- Gillan, F.T., Sandstrom, M.W., 1985. Microbial lipids from a near-shore sediment from Bowling Green Bay, North Queensland: the fatty acid composition of intact lipid fractions. *Org. Geochem.* 8, 321–328.
- Goddéris, Y., Donnadiou, Y., De Vargas, C., Pierrehubert, R.T., Dromart, G., Van De Schootbrugge, B., 2008. Causal or casual link between the rise of nannoplankton calcification and a tectonically-driven massive decrease in Late Triassic atmospheric CO₂? *Earth Planet. Sci. Lett.* 267 (1), 247–255.
- Goossens, H., Rijpstra, W.I.C., Düren, R.R., De Leeuw, J.W., Schenck, P.A., 1986. Bacterial contribution to sedimentary organic matter: a comparative study of lipid moieties in bacteria and recent sediments. *Org. Geochem.* 10, 683–696.
- Gradstein, F.M., Ogg, J.G., Schmitz, M.D., Ogg, G.M., 2012. *The Geologic Time Scale 2012*. Elsevier, Oxford, U.K.
- Graeve, M., Kattner, G., Piepenburg, D., 1997. Lipids in Arctic benthos: does the fatty acid and alcohol composition reflect feeding and trophic interactions? *Polar Biol.* 18, 53–61.
- Guido, A., Jacob, J., Gautret, P., Laggoun-Déferge, F., Mastandrea, A., Russo, F., 2007. Molecular fossils and other organic markers as palaeoenvironmental indicators of the Messinian CdB formation: normal versus stressed marine deposition (Rossano Basin, Northern Calabria, Italy). *Palaeogeogr. Palaeoclimatol. Palaeoecol.* 255, 265–283.
- Guido, A., Mastandrea, A., Tosti, F., Russo, F., 2011. Importance of rare earth element patterns in discrimination between biotic and abiotic mineralization. In: Reitner, J., Quéric, N.V., Arp, G. (Eds.), *Advances in Stromatolite Geobiology*. Lecture Notes in Earth Sciences, 131, pp. 453–462.
- Guido, A., Vescogni, A., Mastandrea, A., Demasi, F., Tosti, F., Naccarato, A., Tagarelli, A., Russo, F., 2012a. Characterization of the micrites in the Late Miocene vermetid carbonate bioconstructions, Salento Peninsula, Italy: record of a microbial/metazoan association. *Sediment. Geol.* 263–264, 133–143.
- Guido, A., Mastandrea, A., Demasi, F., Tosti, F., Russo, F., 2012b. Organic matter remains in the laminated microfabrics of the Kess–Kess mounds (Hamar Laghdad, Lower Devonian, Morocco). *Sediment. Geol.* 263–264, 194–201.
- Guido, A., Mastandrea, A., Rosso, A., Sanfilippo, R., Russo, F., 2012c. Micrite precipitation induced by sulphate reducing bacteria in serpulid bioconstructions from submarine caves (Syracuse, Sicily). *Rend. Online Soc. Geol. Ital.* 21, 933–934.
- Guido, A., Mastandrea, A., Russo, F., 2013a. Biotic vs abiotic carbonates: characterisation of the fossil organic matter with Fourier-transform infrared (FT-IR) spectroscopy. *Boll. Soc. Paleontol. Ital.* 52 (1), 63–70.
- Guido, A., Mastandrea, A., Demasi, F., Tosti, F., Russo, F., 2013b. Preliminary biogeochemical data on microbial carbonatogenesis in ancient extreme environments (Kess–Kess mounds, Morocco). *Riv. Ital. Paleontol. Stratigr.* 119 (1), 19–29.
- Guido, A., Heindel, K., Birgel, D., Rosso, A., Mastandrea, A., Sanfilippo, R., Russo, F., Peckmann, J., 2013c. Pendant bioconstructions cemented by microbial carbonate in submerged marine caves (Holocene, SE Sicily). *Palaeogeogr. Palaeoclimatol. Palaeoecol.* 388, 166–188.
- Haberstroh, P.R., Sansone, F.J., 1999. Reef framework diagenesis across wave-flushed oxic–suboxic–anoxic transition zones. *Coral Reefs* 18, 229–240.
- Hardie, L.A., Bosellini, A., Goldammer, R.K., 1986. Repeated subaerial exposure of subtidal carbonate platforms, Triassic, northern Italy: evidence for high frequency sea-level oscillations on a 10⁴ year scale. *Paleoceanography* 1, 447–457.
- Harris, M.T., 1993. Reef fabrics, biotic crusts and syndepositional cements of the Latemar reef margin (Middle Triassic), Northern Italy. *Sedimentology* 40 (3), 383–401.
- Heindel, K., Birgel, D., Peckmann, J., Kuhnert, H., Westphal, H., 2010. Formation of deglacial microbialites in coral reefs off Tahiti (IODP 310) involving sulfate-reducing bacteria. *Palaios* 25, 618–635.
- Heindel, K., Birgel, D., Brunner, B., Thiel, V., Westphal, H., Gischler, E., Ziegenbalg, S.B., Cabioch, G., Sjövall, P., Peckmann, J., 2012. Post-glacial microbialite formation in coral reefs of the Pacific, Atlantic, and Indian Oceans. *Chem. Geol.* 304–305, 117–130.
- Hummel, K., 1928. Das Problem des Fazieswechsels in der Mitteltrias der Sudtiroler Dolomiten. *Geol. Rundsch.* 19, 223–228.
- Junya, Nan, Congqiang, Liu, Dequan, Zhou, Zhuming, Wang, 2002. REE geochemical study of the Permian–Triassic marine sedimentary environment in Guizhou Province. *Chin. J. Geochem.* 21 (4), 348–361.
- Kamber, B.S., Webb, G.E., 2001. The geochemistry of late Archaean microbial carbonate: implications for ocean chemistry and continental erosion history. *Geochim. Cosmochim. Acta* 65, 2509–2525.
- Kaneda, T., 1991. Iso- and anteiso-fatty acids in bacteria: biosynthesis, function, and taxonomic significance. *Microbiol. Rev.* 55, 288–302.
- Kazmierczak, J., Coleman, M.L., Gruszczynski, M., Kempe, S., 1996. Cyanobacterial key to the genesis of micritic and peloidal limestones in ancient seas. *Acta Paleontol. Pol.* 41, 319–338.
- Keim, L., Schlager, W., 2001. Quantitative compositional analysis of a Triassic carbonate platform (Southern Alps, Italy). *Sediment. Geol.* 139, 261–283.
- Keim, L., Brandner, R., Krystyn, L., Mette, W., 2001. Termination of carbonate slope progradation: an example from the Carnian of the Dolomites, Northern Italy. *Sed. Geol.* 143, 303–323.
- Keim, L., Spötl, C., Brandner, R., 2006. The aftermath of the Carnian carbonate platform demise: a basinal perspective (Dolomites, Southern Alps). *Sedimentology* 53, 361–386.
- Kenter, J.A.M., 1990. Carbonate platform flanks: slope angle and sediment fabric. *Sedimentology* 37, 777–794.
- Kiessling, W., 2010. Reef expansion during the Triassic: spread of photosymbiosis balancing climatic cooling. *Palaeogeogr. Palaeoclimatol. Palaeoecol.* 290, 11–19.
- Knoll, A.H., Bambach, R.K., Payne, J.L., Pruss, S., Fischer, W.W., 2007. Paleophysiology and end-Permian mass extinction. *Earth Planet. Sci. Lett.* 256, 295–313.
- Krull, E.S., Lehrmann, D.J., Druke, D., Kessel, B., Yu, Y.Y., Li, R., 2004. Stable carbon isotope stratigraphy across the Permian–Triassic boundary in shallow marine carbonate platforms, Nanpanjiang Basin, south China. *Palaeogeogr. Palaeoclimatol. Palaeoecol.* 204, 297–315.
- Lawrence, M.G., Greig, A., Collerson, K.D., Kamber, B.S., 2006. Rare earth element and yttrium variability in South East Queensland waterways. *Aquat. Geochem.* 12, 39–72.
- Leonardi, P., 1955. Breve sintesi geologica delle Dolomiti occidentali. *Boll. Soc. Geol. Ital.* 74, 1–140.
- Leonardi, P., 1968. Le Dolomiti. *Geologia dei Monti tra Isarco e Piave*. Consiglio Nazionale delle Ricerche and Giunta Provinciale di Trento. Manfrini, Rovereto, 2 (1019 pp.).
- Logan, G.A., Eglinton, G., 1994. Biogeochemistry of the Miocene lacustrine deposit, at Clarkia, northern Idaho, U.S.A. *Org. Geochem.* 21 (8/9), 857–870.
- Loretz, H., 1875. Einige Petrefakten der alpinen Trias aus den Südalpen. *Z. Dtsch. Geol. Ges.* 27, 784–841.
- Magaritz, M., Krishnamurthy, R.V., Holser, W.T., 1992. Parallel trends in organic and inorganic carbon isotopes across the Permian/Triassic boundary. *Am. J. Sci.* 292, 727–739.
- Martindale, R.C., Zonneveld, J.P., Bottjer, D.J., 2010. Microbial framework in Upper Triassic (Carnian) patch reefs from Williston Lake, British Columbia, Canada. *Palaeogeogr. Palaeoclimatol. Palaeoecol.* 297 (3), 609–620.
- Mastandrea, A., Neri, C., Russo, F., 1997. Conodont biostratigraphy of the S. Cassiano formation surrounding the Sella massif (Dolomites, Italy): implications for sequence stratigraphic models of the Triassic of the southern Alps. *Riv. Ital. Paleontol. Stratigr.* 39–52.
- Mastandrea, A., Barca, D., Guido, A., Tosti, F., Russo, F., 2010. Rare earth element signatures in the Messinian pre-evaporitic Calcarea di Base formation (Northern Calabria, Italy): evidence of normal seawater deposition. *Carbonates Evaporites* 25, 133–143.
- Mastandrea, A., Guido, A., Demasi, F., Ruffolo, S.A., Russo, F., 2011. The characterisation of sedimentary organic matter in carbonates with Fourier-transform infrared (FTIR) spectroscopy. In: Reitner, J., Quéric, N.V., Arp, G. (Eds.), *Advances in Stromatolite Geobiology*. Lecture Notes in Earth Sciences, 131, pp. 331–342.
- Mattavelli, L., Pieri, M., Groppi, G., 1993. Petroleum exploration in Italy: a review. *Mar. Pet. Geol.* 10 (5), 410–425.
- McLennan, S.M., 1989. Rare earth elements in sedimentary rocks: influence of provenance and sedimentary processes. In: Lipin, B.R., McKay, G.A. (Eds.), *Geochemistry and Mineralogy of Rare Earth Elements*. Rev. Mineral. 21, pp. 169–200.
- McRoberts, C.A., Furrer, H., Jones, D.S., 1997. Palaeoenvironmental interpretation of a Triassic–Jurassic boundary section from Western Austria based on palaeoecological and geochemical data. *Palaeogeogr. Palaeoclimatol. Palaeoecol.* 136, 79–95.
- Merz, M.U.E., 1992. The biology of carbonate precipitation by cyanobacteria. *Facies* 26, 81–102.
- Mietto, P., Manfrin, S., Preto, N., Rigo, M., Roghi, G., Furin, S., Gianolla, P., Posenato, R., Muttoni, G., Nicora, A., Buratti, N., Cirilli, S., Spötl, C., Ramezani, J., Bowring, S.A., 2012. The global boundary stratotype section and point (GSSP) of the Carnian stage (Late Triassic) at Prati di Stuares/Stuares Wiesen section (Southern Alps, NE Italy). *Episodes–Newsmagazine of the International Union of Geological Sciences* 35 (3), 414.
- Mojšisovics von Mojvar, E., 1879. Die Dolomit-Riffe von Sudtiroel und Venetien. Alfred Holder, Vienna.
- Monty, C.L.V., 1976. The origin and development of cryptalgal fabrics. In: Walter, M.R. (Ed.), *Stromatolites, Developments in Sedimentology* 20. Elsevier, Amsterdam, pp. 193–249.
- Morante, R., Hallam, A., 1996. Organic carbon isotopic record across the Triassic–Jurassic boundary in Austria and its bearing on the cause of the mass extinction. *Geology* 24 (5), 391–394.
- Müller-Wille, S., Reitner, J., 1993. Palaeobiological reconstruction of selected siphonozoan sponges from the Cassian Beds (Lower Carnian) of the Dolomites (Northern Italy). *Berl. Geowiss. Abh.* 9, 253–281.
- Musashi, M., Isozaki, Y., Koike, T., Kreulen, R., 2001. Stable carbon isotope signature in mid-Panthalassa shallow-water carbonates across the Permo–Triassic boundary: evidence for ¹³C-depleted superocean. *Earth Planet. Sci. Lett.* 191, 9–20.
- Nance, W.B., Taylor, S.R., 1976. Rare earth element patterns and crustal evolution – I. Australian post-Archean sedimentary rocks. *Geochim. Cosmochim. Acta* 40, 1539–1551.
- Neri, C., Gianolla, P., Furlanis, S., Caputo, R., Bosellini, A., 2007. Note Illustrative della Carta Geologica d'Italia alla scala 1:50.000, Foglio 029 Cortina d'Ampezzo. A.P.A.T. SystemCart, Roma 200 pp.
- Neulinger, S.C., Järnegrén, J., Ludvigsen, M., Lochte, K., Dullo, W.C., 2008. Phenotype-specific bacterial communities in the cold-water coral *Lophelia pertusa* (Scleractinia) and their implications for the coral's nutrition, health, and distribution. *Appl. Environ. Microbiol.* 74, 7272–7285.
- Neuweiler, F., Reitner, J., 1995. Epifluorescence microscopy of selected microbialites from Lower Carnian Cipit-boulders of the Cassian Formation (Seeland Alpe, Dolomites). In: Reitner, J., Neuweiler, F. (Eds.), *Mud Mounds: A Polygenetic Spectrum of Fine-grained Carbonate Buildups*. Facies, 32, pp. 26–28.
- Nozaki, Y., Zhang, J., Amakawa, H., 1997. The fractionation between Y and Ho in the marine environment. *Earth Planet. Sci. Lett.* 148, 329–340.
- Ogg, J.G., Ogg, G., Gradstein, F.M., 2008. *The Concise Geologic Time Scale*. Cambridge University Press, U.K.

- Ogilvie, M.M., 1893. Contributions to the Geology of the Wengen and St. Cassian Strata in Southern Tyrol. *Q. J. Geol. Soc. Lond.* 49, 1–78.
- Ogilvie Gordon, M.M., 1927. Das Grödnert-, Fassa- und Enneberggebiet in den Südtiroler Dolomiten. *Abh. der Geol. Bundesanst.* 24 (2), 1–376.
- Ogilvie Gordon, M.M., 1929. Geologie des Gebietes von Pieve (Buchenstein), St. Cassian und Cortina d'Ampezzo. *Jb. Geol. B.-A.* 79 (3–4) (Padova).
- Ott, E., 1966. Die gesteinsbildenden Kalkalgen im Schlauchkar (Karwendelgebirge). *Jahrbuch des Vereins zum Schutze der Alpenpflanzen und -Tiere e. V.* 31 152–159.
- Ouriouss, G., Rohmer, M., Porolla, K., 1987. Prokaryotic hopanoids and other polyterpenoid sterol surrogates. *Annu. Rev. Microbiol.* 41, 301–333.
- Painter, P.C., Snyder, R.W., Starsinic, M., Coleman, M.M., Kuehn, D.W., Davis, A., 1981. Concerning the application of FT-IR to the study of coal: a critical assessment of band assignments and the application of spectral analysis programs. *Appl. Spectrosc.* 35, 475–485.
- Parkes, R.J., Taylor, J., 1983. The relationship between fatty acid distributions and bacterial respiratory types in contemporary marine sediments. *Estuar. Coast. Shelf Sci.* 16, 173–189.
- Perry, G.J., Volkman, J.K., Johns, R.B., Bavor Jr., H.J., 1979. Fatty acids of bacterial origin in contemporary marine sediments. *Geochim. Cosmochim. Acta* 43, 1715–1725.
- Peters, K.E., Walters, C.C., Moldowan, J.M., 2005a. The Biomarker Guide. Volume 1: Biomarkers and Isotopes in the Environment and Human History, Second edition. Cambridge University Press, Cambridge, New York, Melbourne.
- Peters, K.E., Walters, C.C., Moldowan, J.M., 2005b. The Biomarker Guide. Volume 2: Biomarkers and Isotopes in Petroleum Exploration and Earth History, Second edition. Cambridge University Press, Cambridge, New York, Melbourne.
- Pia, J., 1937. Stratigraphie und Tektonik der Dolomiten von Prags., A. Wegeris fb. Hofbuchdruckerei, Wien.
- Piccotti, V., Capozzi, R., Bertozzi, G., Mosca, F., Sitta, A., Tornaghi, M., 2007. The Miocene petroleum system of the Northern Apennines in the central Po Plain (Italy). In: Lacombe, O., Lavé, J., Roure, F., Vergès, J. (Eds.), Thrust Belts and Foreland Basins, From Fold Kinematics to Hydrocarbon System. Springer Verlag, Berlin, pp. 117–131.
- Pond, D.W., Bell, M.V., Harris, R.P., Sargent, J.R., 1998. Microplanktonic polyunsaturated fatty acid markers: a mesocosm trial. *Estuar. Coast. Shelf Sci.* 46, 61–67.
- Powell, T.G., 1988. Pristane/phytane ratio as environmental indicator. *Nature* 333, 604.
- Preto, N., Hinnov, L.A., 2003. Unraveling the origin of carbonate platform cyclothem in the Upper Triassic Dürrenstein Formation (Dolomites, Italy). *J. Sediment. Res.* 73, 774–789.
- Rashid, M.A., 1979. Pristane–phytane ratios in relation to source and diagenesis of ancient sediments from the Labrador Shelf. *Chem. Geol.* 25, 109–122.
- Reitner, J., 1993. Modern cryptic microbialite/metazoan facies from Lizard Island (Great Barrier Reef, Australia): formation and concepts. *Facies* 29, 3–39.
- Richter, C., Wunsch, M., Rasheed, M., Kottler, I., Badran, M.I., 2001. Endoscopic exploration of Red Sea coral reefs reveals dense populations of cavity-dwelling sponges. *Nature* 413, 726–730.
- Richthofen Von, F.F., 1860. Geognostische Beschreibung der Umgegend von Predazzo, Sanct Cassian und der Seisser Alpe in Sud-Tyrol. Justus Perthes, Gotha.
- Riding, R., 2002. Structure and composition of organic reefs and carbonate mud mounds: concepts and categories. *Earth Sci. Rev.* 58, 163–231.
- Riding, R., Liang, L., 2005a. Geobiology of microbial carbonates: metazoan and seawater saturation state influences on secular trends during the Phanerozoic. *Palaeogeogr. Palaeoclimatol. Palaeoecol.* 219, 101–115.
- Riding, R., Liang, L., 2005b. Seawater chemistry control of marine limestone accumulation over the past 550 million years. *Rev. Esp. Micropaleontol.* 37 (1), 1–11.
- Riding, R., Tomás, S., 2006. Stromatolite reef crusts, Early Cretaceous, Spain: bacterial origin of in situ precipitated peloid microspar? *Sedimentology* 53, 23–34.
- Rudolph, K.W., Schlager, W., Biddle, K.T., 1989. Seismic models of a carbonate foreslope-to-basin transition, Picco di Vallandro, Dolomite Alps, northern Italy. *Geology* 17, 453–456.
- Ruhl, M., Kürschner, W.M., Krystyn, L., 2009. Triassic–Jurassic organic carbon isotope stratigraphy of key sections in the western Tethys realm (Austria). *Earth Planet. Sci. Lett.* 281, 169–187.
- Russell, M., Grimalt, J.O., Taberner, C., Rouchy, J.M., 1997. Bacterial and algal inputs in sedimentary organic matter deposited under natural sulphurization conditions (Lorca Basin, Murcia, Spain). *Org. Geochem.* 26, 605–625.
- Russo, F., 2005. Biofacies evolution in the Triassic platform of the Dolomites, Italy. In: Fugagnoli, A., Bassi, D. (Eds.), *Giornate di Studi Paleontologici "Prof. Carmen Loriga Broglio"*. Annali dell'Università degli Studi di Ferrara Museologia Scientifica e Naturalistica. Rastignano, Bologna.
- Russo, F., Neri, C., Mastandrea, A., Laghi, G., 1991. Depositional and diagenetic history of the Alpe di Specie (Seelandalpe) fauna (Carnian, Northeastern Dolomites). *Facies* 25, 187–210.
- Russo, F., Neri, C., Mastandrea, A., Baracca, A., 1997. The mud-mound nature of the Cassian platform margins of the Dolomites. A case history: the Cipit boulders from Punta Grohmann (Sasso Piatto Massif, northern Italy). *Facies* 36, 25–36.
- Salomon, W., 1895. Geologische und paläontologische Studien über die Marmolata. *Paläontographica* 42, 1–210.
- Sánchez-Beristain, J.F., Schäfer, N., Simon, K., Reitner, J., 2011. New geochemical method to characterise microbialites from the St. Cassian Formation, Dolomites, Northeastern Italy. *Lect. Notes Earth Sci.* 131, 435–451.
- Scherer, M., 1977. Preservation, alteration and multiple cementation of aragonitic skeletons from the Cassian Beds (U. Triassic, Southern Alps): petrographic and geochemical evidence. *Neues Jb. Geol. Paläontol. Abh.* 154, 213–262.
- Schlager, W., Keim, L., 2009. Carbonate platforms in the Dolomites area of the Southern Alps – historic perspectives on progress in sedimentology. *Sedimentology* 56, 191–204.
- Schwab, V., Spangenberg, J.E., 2004. Organic geochemistry across the Permian–Triassic transition at the Idrija Valley, Western Slovenia. *Appl. Geochem.* 19, 55–72.
- Scudeler Baccelle, L., 1971. La serie ladino–carnica alla base della Punta Grohmann (Gruppo del Sasso Lungo, Dolomiti occidentali): strutture sedimentarie e petrologia della facies carbonatica. *Memorie Geopaleontologiche dell'Università di Ferrara* 3/2 19–35.
- Sobkowiak, M., Painter, P., 1992. Determination of the aliphatic and aromatic CH contents of coals by FT-IR: studies of coal extracts. *Fuel* 71, 1105–1125.
- Solomon, P.R., Carangelo, R.M., 1988. FT-IR analysis of coal. 2. Aliphatic and aromatic hydrogen concentration. *Fuel* 67, 949–959.
- Stanley Jr., G.D., 1981. Early history of scleractinian corals and its geological consequences. *Geology* 9, 507–511.
- Stanley Jr., G.D., 1988. The history of early Mesozoic reef communities: a three-step process. *Palaios* 3, 170–183.
- Stanley Jr., G.D., 2003. The evolution of modern corals and their early history. *Earth Sci. Rev.* 60, 195–225.
- Stanley Jr., G.D., 2006. Photosymbiosis and the evolution of modern coral reefs. *Science* 312, 857–858.
- Stanley, S.M., Hardie, L.A., 1998. Secular oscillations in carbonate mineralogy of reef-building and sediment-producing organisms driven by tectonically forced shifts in seawater chemistry. *Palaeogeogr. Palaeoclimatol. Palaeoecol.* 144, 3–19.
- Stefani, M., Brack, P., Gianolla, P., Keim, L., Mastandrea, A., Mauer, F., Neri, C., Preto, N., Ragazzi, E., Riva, A., Roghi, G., Russo, F., 2004. Triassic carbonate platforms of the Dolomites (Italy): carbonate production, relative sea-level fluctuations and the shaping of the depositional architecture. 32nd International Geological Congress – Field Trip Guide Book, 20–28 agosto, 2004 (Firenze).
- Stefani, M., Furin, S., Gianolla, P., 2010. The changing climate framework and depositional dynamics of Triassic carbonate platforms from the Dolomites. *Palaeogeogr. Palaeoclimatol. Palaeoecol.* 290, 43–57.
- Tanaka, K., Miura, N., Asahara, Y., Kawabe, I., 2003. Rare earth element and strontium isotopic study of seamount-type limestones in Mesozoic accretionary complex of Southern Chichibu Terrane, central Japan: implication for incorporation process of seawater REE into limestones. *Geochem. J.* 37, 163–180.
- Taylor, J., Parkes, R.J., 1983. The cellular fatty acids of the sulfate-reducing bacteria *Desulfobacter* sp., *Desulfobulbus* sp. and *Desulfovibrio desulfuricans*. *J. Genet. Microbiol.* 129, 3303–3309.
- Thiel, V., Merz-Pfeiß, M., Reitner, J., Michaelis, W., 1997. Biomarker studies on microbial carbonates: extractable lipids of a calcifying cyanobacterial mat (Everglades, USA). *Facies* 36, 163–172.
- Tissot, B.P., Welte, D.H., 1984. Petroleum Formation and Occurrence. Second Revised and Enlarged Edition. Springer-Verlag, Berlin, Heidelberg, New York.
- Tosti, F., Guido, A., Demasi, F., Mastandrea, A., Naccarato, A., Tagarelli, A., Russo, F., 2011a. Microbialites as primary builders of the Ladinian–Carnian platforms in the Dolomites: biogeochemical characterization. *Geol. Alp.* 8, 156–162.
- Tosti, F., Guido, A., Demasi, F., Mastandrea, A., Russo, F., 2011b. Biogeochemical characterization of automicrites building the Cipit Boulders of the Ladinian–Carnian platforms in the Dolomites (northeastern Italy). *Rend. Online Soc. Geol. Ital.* 17, 179–183.
- Tosti, F., Guido, A., Mastandrea, A., Demasi, F., Russo, F., 2012. Rare earth elements signature in Triassic samples from Punta Grohmann and Alpe di Specie (Dolomites, Italy): evidence of cyanobacterial vs sulfate reducing bacteria metabolic activities. *Rend. Online Soc. Geol. Ital.* 21, 943–944.
- Tucker, M.E., Hollingworth, N.T.J., 1986. The Upper Permian reef complex (EZ) of north east England. In: Shroeder, J.H., Purser, B.H. (Eds.), *Reef Diagenesis*. Springer Verlag, Berlin.
- Van Kranendonk, M.J., Hugh Smithies, R., Hickman, A.H., Champion, D.C., 2007. Review: secular tectonic evolution of Archean continental crust: interplay between horizontal and vertical processes in the formation of the Pilbara Craton, Australia. *Terra Nova* 19 (1), 1–38.
- Viso, A.C., Marty, J.C., 1993. Fatty acids from 28 marine microalgae. *Phytochemistry* 34, 1521–1533.
- Volkman, J.K., Jeffrey, S.W., Nichols, P.D., Rogers, G.I., Garland, C.D., 1989. Fatty acid and lipid composition of 10 species of microalgae used in mariculture. *J. Exp. Mar. Biol. Ecol.* 128, 219–240.
- Wakeham, S.G., 1995. Lipid biomarkers for heterotrophic alteration of suspended particulate organic matter in oxygenated and anoxic water columns of the ocean. *Deep-Sea Res.* 1 42, 1749–1771.
- Wakeham, S.G., Beier, J.A., 1991. Fatty-acid and sterol biomarkers as indicators of particulate organic matter source and alteration processes in the Black Sea. *Deep-Sea Res.* 38, 943–968.
- Wang, S.H., Griffiths, P.R., 1985. Resolution enhancement of diffuse reflectance I.R. spectra of coals by Fourier-self deconvolution. 1. C–H stretching and bending modes. *Fuel* 64, 229–236.
- Webb, G.E., 1996. Was Phanerozoic reef history controlled by the distribution of non-enzymatically secreted reef carbonates (microbial carbonate and biologically induced cement)? *Sedimentology* 43, 947–971.
- Webb, G.E., Kamber, B.S., 2000. Rare earth elements in Holocene reefal microbialites: a new shallow seawater proxy. *Geochim. Cosmochim. Acta* 64, 1557–1565.
- Weidlich, O., Bernecker, M., Flügel, E., 1993. Combined quantitative analysis and microfacies studies of ancient reefs: an integrated approach to Upper Permian and Upper Triassic reef carbonates (Sultanate of Oman). *Facies* 28, 115–144.
- Wendt, J., 1974. Der Skelettbau aragonitischer Kalkschwämme aus der alpinen Obertrias. *Neues Jahrbuch für Geologie und Paläontologie, Monatshefte* 8, 498–511.
- Wendt, J., 1975. Aragonitische Stromatoporen aus der alpinen Obertrias. *N. Jb. geol. paläont. Abh.* 150 (1), 111–125.
- Wendt, J., 1977. Aragonite in Permian Reefs. *Nature* 267, 335–337.

- Wendt, J., 1982. The Cassian patch reefs (Lower Carnian, Southern Alps). *Facies* 6, 185–202.
- Wendt, J., Fürsich, F.T., 1980. Facies analysis and paleogeography of the Cassian Formation, Triassic, Southern Alps. *Riv. Ital. Paleontol. Stratigr.* 85, 1003–1028.
- Werner, U., Bird, P., Wild, C., Ferdelman, T., Polerecky, L., Eickert, G., Johnstone, R., Hoegh-Guldberg, O., deBeer, D., 2006. Spatial variability of aerobic and anaerobic mineralization in coral reef sediments (Heron Island, Australia). *Mar. Ecol. Prog. Ser.* 309, 93–105.
- Whalen, M.T., Beatty, T.W., 2008. Kamishak Formation, Puale Bay. In: Reifensstuhl, R.R., Decker, P.L. (Eds.), *Bristol Bay–Alaska Peninsula Region, Overview of 2004–2007 Geologic Research: Alaska Division of Geological and Geophysical Surveys Report of Investigation 2008-1G*, pp. 105–129.
- Wood, R., 1998. The ecological evolution of reefs. *Annu. Rev. Ecol. Evol. Syst.* 29, 179–206.
- Wood, R., Dickson, J.A.D., Kirkland-George, B., 1994. Turning the Capitan reef up-side down: a new appraisal of the ecology of the Permian Capitan Reef, Guadalupe Mountains, Texas and New Mexico. *Palaeos* 9, 422–427.
- Wood, R., Dickson, J.A.D., Kirkland-George, B., 1996. New observations on the ecology of the Permian Capitan Reef, Guadalupe Mountains, Texas and New Mexico. *Palaeontology* 39, 733–762.
- Yin, Hongfu, Xie, Shucheng, Yan, Jiaxin, Chaoyong, Hu, Junhua, Huang, Tenger, Qie, Wenkun, Qiu, Xuan, 2011. Geobiological approach to evaluating marine carbonate source rocks of hydrocarbon. *Sci. China Earth Sci.* 54 (8), 1121–1135.
- Zankl, H., 1969. Der Hohe Göll. Aufbau und Lebensbild eines Dachstein-Riffes in der Obertrias der nördlichen Kalkalpen. *Abhandlungen der Senckenbergischen Naturforschenden Gesellschaft*, 519 1–123.
- Zankl, H., Müller, H.R., 1977. Origin of some internal fabrics in Holocene reef rocks, St. Croix, US Virgin Islands. *Proceedings of the Third International Coral Reef Symposium* 2, pp. 127–133.
- Zonneveld, J.P., Henderson, C.M., Stanley Jr., G.D., Orchard, M.J., Gingras, M.K., 2007. Oldest scleractinian coral reefs on the North American craton: Upper Triassic (Carnian), northeastern British Columbia, Canada. *Palaeogeogr. Palaeoclimatol. Palaeoecol.* 243, 421–450.